Neural control of breathing In Parkinson's disease: an exploratory study

A master's thesis for the degree of Technical Medicine

By Marit Lisanne Schuurbiers

22 March 2024, Nijmegen

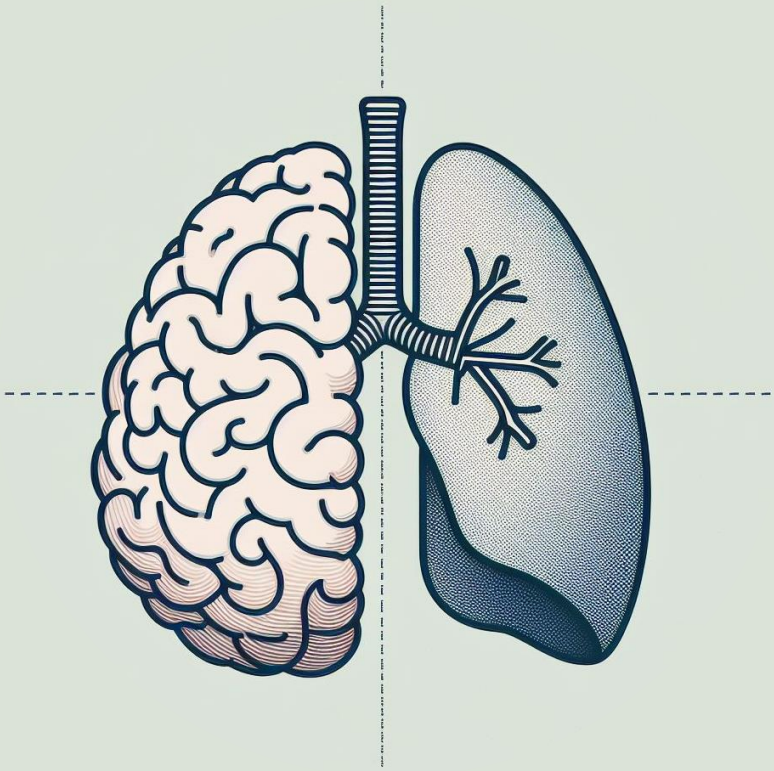

UNIVERSITY OF TWENTE.

Radboudumc

Abstract

Introduction

Parkinson's disease (PD) is a progressive neurological movement disorder, with up to 40% of individuals with PD experiencing respiratory dysfunction. However, the exact mechanisms of respiratory dysfunction in PD remain unknown. The complex process of neural control of breathing may be involved, but this is still understudied. This study aims to fill this gap. The main objective of this study is to identify PD specific alterations in neural control of breathing by using advanced respiratory neurophysiological techniques.

Methods

We performed an exploratory observational cross-sectional study in subjects with PD and healthy controls, using three measurements: the hypercapnic ventilatory response (HCVR), transcranial magnetic stimulation (TMS) and respiratory related evoked potentials (RREP). The HCVR measured the chemosensitivity to the partial pressure of carbon dioxide (PCO_2). TMS was used to evaluate cortical excitability of the motor pathways to the diaphragm. The RREP gave an indication of how the brain processes respiratory sensations.

Results

We included 9 healthy controls and 4 subjects with mild to moderate PD, who continued their dopaminergic medication. Chemosensitivity, as measured with HCVR, was unaffected in subjects with PD. Cortical excitability of the diaphragm, as assessed with TMS, was higher in subjects with PD. The RREP showed attenuated first-order and cognitive processing in the perception of respiratory sensations for subjects with PD. Results were not statistically significant.

Conclusion

This study provides new insights into the neural control of breathing in PD. Despite the limited sample size, the findings collectively indicate that both the motor and sensory pathways involved in neural control of breathing are impaired in individuals with mild to moderate PD on dopaminergic medication, whilst the chemosensitivity to PCO_2 remains intact. These findings suggest that neural control of breathing is impaired in PD. This is a significant step forward in our understanding of this disease. Whilst further research is still necessary, a better understanding of neural control of breathing in PD can ultimately lead to new treatments to respiratory dysfunction.

Graduation committee

Chairman	prof.dr. D.W. Donker MD
Clinical/Daily supervisor	dr. J. Doorduin
Technical supervisor	dr. E. Mos-Oppersma
Process supervisor	dr. M. Groenier
External member	S. Stuiver, MSc.

List of abbreviations

BMI	Body mass index
CNS	Central nervous system
COPD	Chronic pulmonary obstructive disease
EEG	Electroencephalography
EMG	Electromyography
EP	Evoked potentials
FEV_1	Forced expiratory volume in 1 second
FiO_2	Fraction of inspired O_2
FVC	Forced vital capacity
HCVR	Hypercapnic ventilatory response
ICS	Intercostal space
ISI	Interstimulus interval
M	Musculus
MEP	Maximal expiratory pressure
MEP	Motor evoked potential
MIP	Maximal inspiratory pressure
PAT	Projected apnoea threshold
PCO_2	Partial pressure of carbon dioxide
PD	Parkinson's disease
$PetCO_2$	End tidal PCO_2
PO_2	Partial pressures of oxygen
RAR	Rapidly adapting stretch receptor
RMT	Resting motor threshold
RREP	Respiratory related evoked potential
SAR	Slowly adapting stretch receptor
SNIP	Sniff nasal inspiratory pressure
TMS	Transcranial magnetic stimulation
VRT	Ventilatory recruitment threshold

Table of contents

Abstract 1
Graduation committee 2
List of abbreviations 2
1. Introduction 5
2. Background 7
2.1 Neural control of breathing 7
2.2 Parkinson's disease 8
2.3 Respiratory dysfunction in Parkinson's disease 8
2.4 Monitoring methods 9
2.4.1 Hypercapnic ventilatory response 9
2.4.2 Transcranial magnetic stimulation 9
2.4.3 Respiratory related evoked potential 10
3. Methods 11
3.1 Study design 11
3.2 Study population 11
3.3 Study procedures 12
3.3.1 Baseline characteristics 12
3.3.2 Hypercapnic ventilatory response curve 12
3.3.3 Transcranial magnetic stimulation 12
3.3.4 Respiratory related evoked potential 13
3.4 Data acquisition 14
3.4.1 Hypercapnic ventilatory response curve 14
3.4.2 Transcranial magnetic stimulation 14
3.4.3 Respiratory related evoked potential 14
3.5 Data analysis 15
3.5.1 Hypercapnic ventilatory response curve 15
3.5.2 Transcranial magnetic stimulation 16
3.5.3 Respiratory related evoked potential 16
3.6 Statistical analysis 18
4. Results 19
4.1 Subject characteristics 19
4.2 Hypercapnic ventilatory response 19
4.3 Transcranial magnetic stimulation 21
4.4 Respiratory related evoked potentials 26
5. Discussion 29

5.1 Pulmonary function 29
5.2 Hypercapnic ventilatory response 29
5.3 Transcranial magnetic stimulation 30
5.4 Respiratory related evoked potential 31
5.5 Integration of the findings 32
5.4 Limitations 33
6. Conclusion 35
References 36
Appendix A: Neural control of breathing 39
Appendix B: Additional results 42
Subject characteristics 42
Pulmonary function 43
Respiratory related evoked potential 43

1. Introduction

Parkinson's disease (PD) is a progressive neurological movement disorder [1], [2]. It is the second most common neurodegenerative disorder, after Alzheimer's disease, and affects about 1% of people over the age of 65 in all countries [2]. Loss of dopaminergic cells in the regions of the brain associated with movement causes motor symptoms in patients with PD, such as tremor, dyskinesia and rigidity. Less is known about respiratory dysfunction in PD, even though it leads to debilitating symptoms, such as dyspnoea or coughing difficulties.

Up to 40% of individuals with PD experience respiratory dysfunction [3]. Moreover, evidence suggests that respiratory dysfunction can lead to pneumonia, which is a complication in late-stage PD and a strong predictor of death [4], [5], [6]. There are two points of interest with regards to respiratory dysfunction: peripheral and central problems. The peripheral mechanisms include defects in motor function that limit sufficient ventilation, such as rigidity of the thorax and weakness of the respiratory muscles that both limit the expansion of the lungs. Central problems in respiratory dysfunction refers to the inability of the central nervous system to adequately control breathing, regardless of limitations of the motor function. Neural control of breathing is a complex process that involves control of the respiratory muscles through the brainstem. This automatic process is influenced by changes in metabolic demands, which include changes in arterial partial pressures of oxygen (PO_2), carbon dioxide (PCO_2) and in pH, and by changes in mechanical conditions, for example when changing posture. Control of breathing is also influenced by voluntary cortical commands, such as consciously holding one's breath.

The involvement of deficits in the central nervous system (CNS) in respiratory dysfunction in Parkinson's disease is still relatively unknown. Several studies have proposed that there is early impairment of respiratory control centres in PD, because respiratory dysfunction can occur before motor symptoms are present [7]. This is in part expressed as an abnormal perception of dyspnoea and an abnormality of the central respiratory drive [3], [8], [9], [10], [11]. These studies have mainly been focused on measuring the change in ventilation in response to a hypoxic or hypercapnic stimulus. There is evidence that the dopaminergic cells involved in sensing PO_2, PCO_2 and pH are affected in the early stages of PD, which can lead to an abnormal chemosensitivity to hypoxia and hypercapnia [3], [8], [9], [12]. There is, however, still a lack of knowledge about the exact mechanisms of abnormal neural control of breathing in PD. This is partly caused by methodological limitations to quantify neural control of breathing.

In this study, we use neurophysiological methods to assess the central mechanisms underlying respiratory dysfunction in PD. Recently, advanced techniques have been explored at the Radboud University Medical Center (Radboudumc) that can assess the neural mechanisms underlying the central problems in respiratory dysfunction. Three techniques will be used in this study: hypercapnic ventilatory response (HCVR) curve, transcranial magnetic stimulation (TMS) of the diaphragm and respiratory related evoked potentials (RREP). All three methods consider a different part of the mechanism of neural control of breathing. The HCVR measures the response in ventilation to change in PCO_2 [13]. TMS uses magnetic pulses to stimulate the motor cortex, which generates a potential in the diaphragm [14]. It is used to evaluate cortical excitability with regards to breathing. The RREP is a characteristic pattern in brain activity in response to a short inspiratory occlusion [15]. It can be used

to evaluate how the brain processes respiratory sensations. Together, these three techniques will provide as complete a picture as possible of the central impairment in respiratory dysfunction. This will expand our knowledge of the mechanisms of respiratory dysfunction in patients with PD. When these mechanisms are better understood, future treatments could target the impaired mechanisms better.

The main objective of this study is to identify disease (Parkinson's disease) specific alterations in neural control of breathing by using respiratory neurophysiological techniques. We will test the hypothesis that neural control of breathing is impaired in patients with PD with mild to moderate disease stage and on dopaminergic medication, compared to healthy age-matched controls. More specifically, regarding the different neurophysiological techniques, we hypothesise that in PD the hypercapnic response is reduced, that there is an increased cortical excitability of the diaphragm and that the RREP components are less frequently present or reduced in amplitude.

Our hypotheses are based on different previous observations. Firstly, that there is a decrease of chemosensitive neurons in the brainstem in both humans with PD and animal studies with modelled PD [12], reducing the ability to detect changes in metabolic demand. Secondly, earlier studies found an altered response to hypercapnia and hypoxia in patients with PD [8], [12]. Thirdly, a study of TMS in PD concluded that patients with PD show an enhanced corticospinal motor output at rest, resulting from a reduction in intracortical inhibition, and a reduction of voluntary facilitation [16], [17]. We expect the same effect when the stimulation is targeted at the diaphragm. Lastly, a previous finding of a study shows impaired cortical processing of afferent respiratory signals in children with chronic ventilatory defects [18]. The inability of these children to detect a change in respiratory load, as seen by the absence of RREP components, is likely caused by the higher load that they experience during respiration in a normal situation. Assuming that patients with PD also breathe with higher load for a longer period of time, caused by for example their rigidity of the chest wall, the RREPs might show reduction or even absence of amplitudes of the RREP components.

2. Background

2.1 Neural control of breathing

To understand the changes in neural control of breathing in PD, the normal mechanisms of control of breathing will be discussed. The goal of breathing is to achieve a homeostatic regulation of the pH and arterial oxygen and carbon dioxide levels [19]. It is a complex process that involves many elements. A simplified and schematic overview of the pathway of neural control of breathing is shown in Figure 1. Rhythmic contraction of the respiratory muscles normally occurs automatically. Neurons in the medulla, located within the brainstem, generate signals that travel via the phrenic nerve to the diaphragm and via the intercostal nerves to the intercostal muscles. In the muscles, motor units are recruited and the firing rate is increased. This leads to contraction of the muscles, which expands the thoracic cavity and creates a more negative pressure. This causes air to flow into the lungs so alveolar ventilation can take place. Oxygen in the alveoli diffuses into the alveolar capillaries and carbon dioxide diffuses from the capillaries into the alveolar air. This changes PO_2 and PCO_2.

Central and peripheral chemoreceptors monitor PO_2, PCO_2 and pH. The central chemoreceptors are located in the brainstem and can sense changes in arterial PCO_2 and pH. The peripheral chemoreceptors are located in the carotid bodies in the neck and the aortic bodies in the thorax and are mostly sensitive to changes in PO_2, but can also detect fluctuations in PCO_2 and pH. The information, from the upper airways, is sent through the glossopharyngeal nerve (CN IX).

Mechanical receptors in the lungs and the chest wall also detect changes in breathing parameters [19], [20]. Two types of pulmonary stretch receptors exist in the lungs: slowly adapting stretch receptors (SARs) and rapidly adapting stretch receptors (RARs). The SARs are stimulated by stretch and adapt slowly to a change in lung volume. RARs are stimulated by both chemical and mechanical stimuli and respond to lung deflation. Another type of pulmonary receptors is the C fibres. These are located deep within the lungs. It is believed that these receptors are responsive to the degree of distention of the interstitium and are therefore responsive to mechanical stimulation. This information from the lungs and lower airways is sent through the vagal nerve (CN X). All sensory feedback, both from the mechanical receptors and the peripheral chemoreceptors, is integrated and conveyed to the medulla.

Other important stretch receptors are muscle spindles in the chest wall. They notice changes in airway resistance and respiratory system compliance. They are located in the skeletal muscles: mainly in the intercostal muscles, but also in the diaphragm to a lesser extent [20]. The information from the muscle spindles is sent through the spinal cord, via the spinal nerves, and is conveyed to the somatosensory cortex.

Breathing is also partly regulated by voluntary control, for example during talking, swallowing and diving. This is initiated in the motor cortex and these signals are also relayed to the medulla, which can alter contraction of the respiratory muscles.

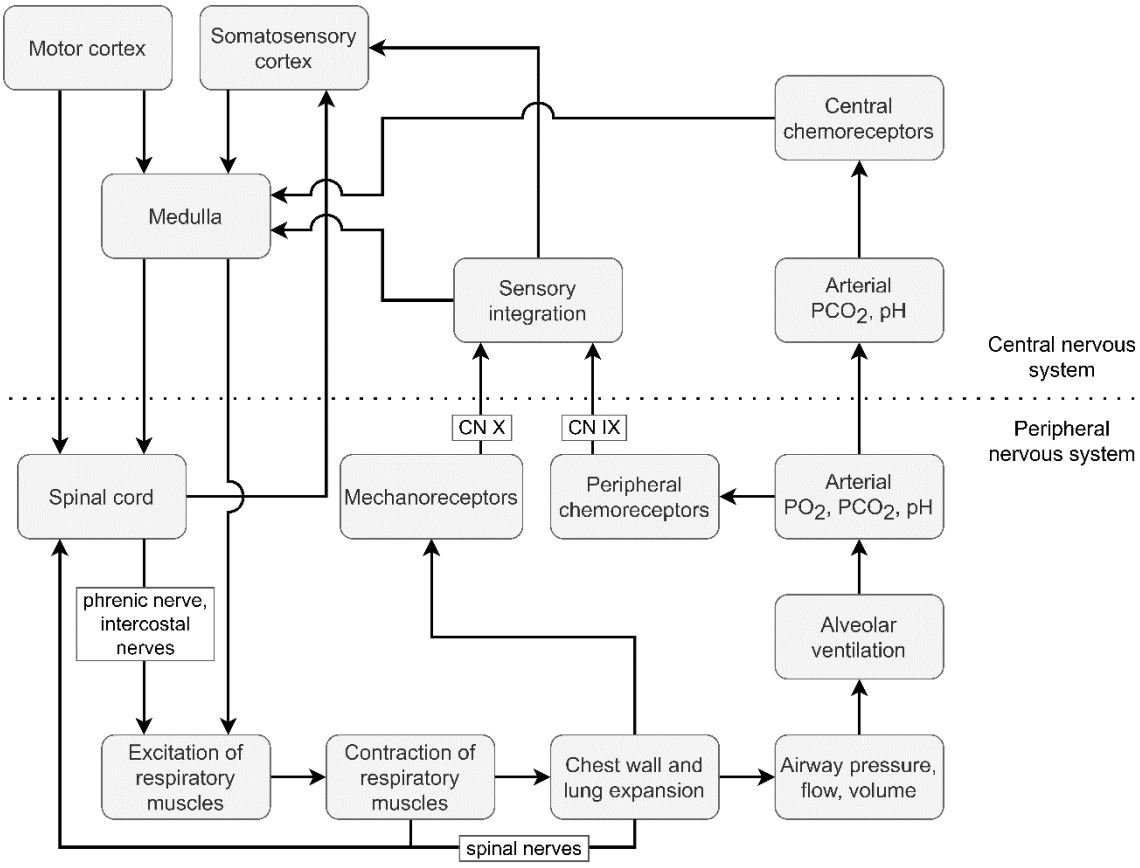

Figure 1 Simplified scheme of neural control of breathing. CN X: vagal nerve, CN IX: glossopharyngeal nerve, PO_2: partial pressure of O_2, PCO_2: partial pressure of CO_2.

2.2 Parkinson's disease

Dopamine is a crucial neurotransmitter, being responsible for the regulation of movement. In PD, dopaminergic neurons are progressively lost, causing various symptoms in patients. Common symptoms are tremor, bradykinesia, rigidity and postural instability. These defects in motor function are caused by the loss of dopaminergic neurons of the basal ganglia, which are a collection of nuclei in the midbrain and are associated with the control of voluntary movement [19].

Two pathways are involved in the control of movement: the direct pathway that generates movement and the indirect pathway that prevents unwanted movement. In healthy individuals, the dopamine containing neurons in the substantia nigra of the basal ganglia initiate more movement in the direct pathway and prevent excessive reduction in movement in the indirect pathway [1], [19], [21]. The degeneration of dopaminergic neurons in PD reduces these functions of the substantia nigra and causes suppression of movement in both the direct and indirect pathway. This results in the common movement symptoms of PD.

2.3 Respiratory dysfunction in Parkinson's disease

Patients with PD often experience respiratory dysfunction. Symptoms differ from the feeling of dyspnoea to difficulty with swallowing or coughing. The respiratory dysfunction can originate from a peripheral or central cause, or a combination of both. Peripheral problems include restrictive and

obstructive dysfunction. The restrictive mechanism may be caused by bradykinesia and rigidity, which limit expansion of the thorax during respiration [10]. Muscle weakness and tremor of the inspiratory muscles may also cause the restrictive pattern of the respiratory dysfunction [9]. As a result, the vital capacity of the lungs decreases, which may lead to a decrease in oxygenation. This can increase the perception of dyspnoea. Obstructive dysfunction is characterised as an obstruction of either the upper or lower airways [3], [8], [9], [10]. It is associated with symptoms such as stridor, wheezing and decreased expiratory flow.

2.4 Monitoring methods

Respiration can be measured in many different ways. The pulmonary function itself can be investigated by means of spirometry, for example, and the blood gas tensions that play an important role in control of breathing can be measured with an arterial blood sample. More challenging is the measurement of the control of breathing by the CNS. Several techniques have been researched that can help understand the involvement of neural control in respiratory dysfunction.

2.4.1 Hypercapnic ventilatory response

The HCVR curve measures the hypercapnic response. The hypercapnic response is the response in ventilation to a change in PCO_2 [13], [22]. In Appendix A (Figure 12), the components of the neural control of breathing that are measured with the HCVR are indicated. The arterial PCO_2 and the pH are sensed by peripheral chemoreceptors in the carotid body and the chemoreceptors in the medulla. These signals result in a response in alveolar ventilation by controlling the respiratory muscles. The HCVR provides information about the feedback of the central chemoreceptors that regulate control of breathing, which is an important aspect of the neural control. In this study, the HCVR will be determined by using a CO_2-rebreathing technique. The arterial PCO_2 is estimated by the end tidal PCO_2 ($PetCO_2$) and arterial ventilation is approximated by the minute ventilation. A linear regression model is fitted through the data, resulting in a curve that shows the relationship between PCO_2 and minute ventilation: the HCVR. The model is assumed to be linear above the ventilatory recruitment threshold (VRT). At PCO_2 levels below VRT, chemoreceptors are not sensitive to PCO_2 changes. Breathing is then assumed to be driven by basal ventilation. The PCO_2 level where, hypothetically, ventilation ceases completely is called the projected apnoea threshold (PAT). The term “projected” means that it only exists in individuals that are asleep.

2.4.2 Transcranial magnetic stimulation

In TMS, magnetic pulses activate the motor cortex, which generates a motor evoked potential (MEP) in the corresponding target muscle [14], [23]. It is a useful tool for assessment of corticospinal excitability of the motor pathways to the target muscle. The MEP response is recorded using surface electromyography (EMG) electrodes that are placed on the target muscle. Stimulus response curves can be used to assess the input output characteristics of corticospinal pathways, both at rest and during different levels of voluntary facilitation. The effect of a subthreshold conditioning stimulus on a suprathreshold test stimulus provides information about the excitability of intracortical inhibitory and excitatory circuits. When the interstimulus interval is short there is inhibition mediated by GABA-A receptors. At longer intervals, the effect is facilitatory and is thought to be mediated by the activation of cortico-cortical pyramidal cells and their axons, which have excitatory glutaminergic synapses. This study will use TMS to stimulate the diaphragm, as this gives insight in the cortical

excitability, with regards to breathing. The relation between TMS and neural control of breathing is outlined in Appendix A (Figure 13).

2.4.3 Respiratory related evoked potential

Perception and processing of respiratory sensations are an essential aspect of neural control. RREPs can be used to evaluate how the brain processes respiratory input signals. An electroencephalogram (EEG) is used to assess the signals of the brain. When a specific population of neurons in the cortex are activated, a group of cortical neurons depolarises [1], [15]. This creates a dipole, where a positive and negative charge are separated by a distance. The EEG records the current from these dipoles. The polarity is related to the orientation of the group of cortical neurons and the location and the location of the reference electrode. The amplitude is directly proportional to the number of depolarised cells. The EEG can also record evoked potentials (EP). An EP is specific electrical activity in the brain or spinal cord in response to certain stimuli. Common stimuli are auditory, visual or somatosensory cues. A RREP is a specific, respiratory, EP, that can be induced by a short inspiratory occlusion of breathing [15]. The occlusion elicits a specific pattern in brain activity, as illustrated in Figure 2 [24]. The mechanism is not entirely understood, but it is believed that the occlusion triggers mechanoreceptors in the airways, lungs, chest wall and respiratory muscles and elicits a somatosensory stimulation of the respiration. The RREP indicates arrival of the sensory information to the brain and shows the further processing in the cortex. The pathway of the RREP in the neural control of breathing is shown in Appendix A (Figure 14). The RREP is characterised by several peaks (Figure 2). The early peaks (Nf, P1, N1) have a latency smaller than 130 ms post stimulus. These components reflect the initial arrival and first-order processing of the afferent respiratory signals in the sensory motor cortex. The later components (P2, P3) that occur more than 150 ms after the onset of the stimulus, reflect second order cognitive processing. The amplitudes of P2 and P3 are related to the sensation of respiratory stimuli [25], [26]. Increased amplitudes could reflect that the respiratory sensations are perceived as more aversive and motivationally relevant. This is valuable in this study, as greater perception of respiratory sensations is related to an increased feeling of dyspnoea, which patients with PD experience as well. In short, RREP measurements in patients with PD could provide an objective estimate of the capacity to detect changes in respiratory mechanics [18].

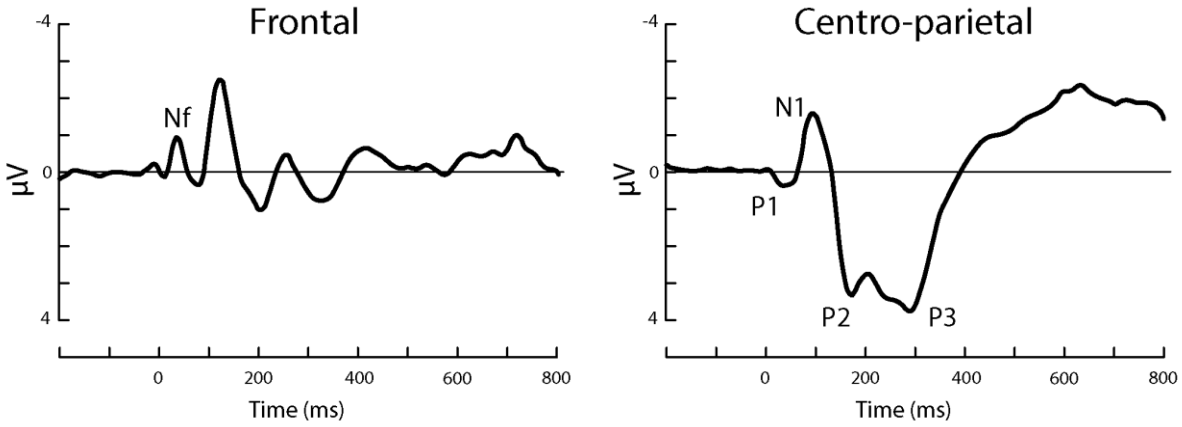

Figure 2 Illustrative example of a respiratory related evoked potential (RREP). The frontal component (Nf) is shown on the left and the centro-parietal components (N1, P1, P2 and P3) are shown on the right. Note that the y-axis is reversed. From "Cortical sources of the respiratory related evoked potential" by Von Leupoldt, A. et al. 2010. Respiratory physiology & neurobiology, *170(2), 198-201.*

3. Methods

This study compares the mechanism of neural control of breathing in healthy controls and individuals with PD. As this research falls under the Medical Research Involving Human Subjects Act (WMO), it had to be reviewed by an independent committee of experts. This study has been approved by the local Medical Research Ethics Committee (METC Oost-Nederland) and has been registered as *NL84745.091.23*. In this thesis, the preliminary results of the first fourteen participants are presented.

3.1 Study design

This study is an exploratory observational cross-sectional study in subjects with PD and healthy controls. The aim was to match subjects with PD to the healthy controls, based on age and sex. All measurements were performed during a one-day visit at the Department of Neurology at the Radboudumc in Nijmegen.

3.2 Study population

Healthy controls were recruited via advertisements on flyers and the SONA system, which is a digital database for people interested in participating in research connected to the Donders Institute.

For the inclusion of subjects with PD, we reached out to individuals who had previously been screened for another study and had approved contact for later studies. All patients had a confirmed diagnosis of PD with Hoehn and Yahr staging 1 to 3. This scale is used for the degree of functional disability and is intended for monitoring progression of the disease [27]. Staging 1 to 3 includes patients with mild to moderate disease, ranging from unilateral involvement only in stage 1, to mild to moderate bilateral involvement, some postural instability but physically independent in stage 3. Inclusion of a maximal stage of 3 will reduce the influence of heavy motor symptoms, as these get more pronounced in even later stages of PD. They were asked to take their dopaminergic medication, such as levodopa, as usual. We only included subjects without a pre-existing pulmonary disease, meaning that they had to have normal pulmonary function. This was especially important for the subjects with PD. Any potential abnormal findings in the respiratory physiological measurements could only be exclusively attributed to impaired neural control of breathing, when pulmonary function was only minimally compromised. The exclusion criteria for all participants are listed below.

- Age younger than 18 years
- Healthy controls: previous or ongoing diseases of the central nervous system
- Patients: previous or ongoing diseases of the central nervous system, other than Parkinson's disease
- History of or current psychiatric treatment
- History of or current brain surgery or epilepsy, including deep brain stimulation
- Neuromuscular disorders
- Pre-existing pulmonary disease, such as chronic obstructive pulmonary disease, asthma or pulmonary fibrosis
- TMS incompatibility (metal parts in head or neck, skin allergies)
- Implanted cardiac pacemaker or defibrillator, neurostimulator, cochlear implant or medical infusion device
- Large or ferromagnetic metal parts in the head (except for a dental wire)
- Pregnancy
- Smoking

3.3 Study procedures

3.3.1 Baseline characteristics

Baseline characteristics of all subjects were collected, including age, gender, height, weight, medication and smoking and alcohol history. Study parameters for patients only, are the age at disease onset, duration of the disease and Hoehn and Yahr disease stage.

Pulmonary function was assessed for every participant. A standard clinical pulmonary function test was performed using hand-held devices (Pneumotrac Spirometer with RMS, model 6800, with Spirotrac 6 Software, Vitalograph, Ennis, Co. Clare, Ireland). The forced vital capacity (FVC), forced expiratory volume in 1 second (FEV1), peak expiratory flow (PEF), maximal inspiratory pressure (MIP), maximal expiratory pressure (MEP) and the sniff nasal inspiratory pressure (SNIP) were obtained.

3.3.2 Hypercapnic ventilatory response curve

The HCVR was determined using the CO_2 rebreathing test [22]. Subjects breathed into a system through a face mask, covering their nose and mouth (Hans Rudolph, Shawnee, KS, USA). To maintain a one-way circuit, a y-piece with valves for inspiration and expiration was placed in the system. Flow, mouth pressure, PCO_2 and PO_2 were recorded during the entire test. During the first phase of the test, the breathing system remained open, so the subject could inhale room air and baseline ventilation could be determined. After two minutes, the system was closed. The inspiratory and expiratory valves were connected to a twenty-litre rebreathing bag (Vyaire Medical, Mettawa, IL, USA) that had been filled with oxygen before the test to keep FiO_2 above 35%. During the rebreathing phase, inspiratory PCO_2 was continuously raised by exhalation of the subject in the closed system and inhaling that same air. If $PetCO_2$ reached > 8.5 kPa or if the subject indicated that they would like to stop, the rebreathing phase was ended by switching the system back to an open system. The subject remained connected to the system until ventilation and PCO_2 reached baseline level, thereby measuring the recovery phase.

3.3.3 Transcranial magnetic stimulation

The TMS study protocol was based on the protocol of Chakalov et al., who determined the ideal parameters for TMS of the diaphragm [14]. In the current study we used an identical TMS device and coil, as well as the same placement of the EMG electrodes.

TMS was delivered over the motor cortex using a magnetic stimulator and a 2 x 97 mm butterfly coil (MagVenture MC B70) with an interval of at least 30 seconds between stimulations. Stimuli were delivered using a MagVenture device (MagPro model X100 including MagOption). EMG of the respiratory muscles was recorded using surface electrodes on the chest wall. Initially, the goal was to stimulate the motor cortex on the left side of the head and to record EMG activity on the right side. For one subject, the stimulation was switched to the right side and the EMG electrodes were placed on the left side.

A short diaphragm EMG lead was placed on both sides and a long diaphragm EMG lead was placed contralateral to stimulation. For the short electrode, the active electrode was placed between the costochondral junction and the midclavicular line (MCL) in the 7^{th}, 8^{th} or 9^{th} intercostal space (ICS). The reference electrode was placed on the rib above, slightly lateral to the active electrode. For the long

diaphragm EMG lead, the reference electrode was placed 5 cm above the xiphoid process and the active electrode was positioned at a 16 cm distance from the reference electrode, directly below the ribcage. To ensure that the observed MEP was a result of contraction of the diaphragm and not the neighbouring muscles, additional EMG leads were used. One pair of electrodes was used to record activity from the musculus (M.) latissimus dorsi and the M. serratus anterior, positioned in the 6th ICS at the posterior axillary line contralateral to stimulation. Another pair was used to register activity of the M. rectus and the M. transversus abdominus, approximately 4 cm below the ribcage on the contralateral side to stimulation.

Electrode position was confirmed by electrical stimulation (DS7A High Voltage Constant Current Stimulator, Hertfordshire, UK) of the phrenic nerve on the right side of the neck. The MEPs in the long and short diaphragmatic EMG were observed. Electrode position was optimised based on the location of the electrodes that resulted in the highest MEP amplitude.

The motor hotspot of the diaphragm was determined by stimulating over the motor cortex on the left side of the head. Cz, Fz and C3 were marked on the subject's head, using the international 10-20 EEG placement system. As the motor hotspot of the diaphragm was expected to be located between these points, the TMS-search started along the projected grid between Cz, Fz and C3. TMS stimulations were performed at 70 to 90% of stimulator intensity until a response in the EMG of the diaphragm was observed. In some instances, a distinct response was not observed. This could be due to either a barely visible MEP or excessive co-stimulation of neighbouring muscles that hindered the isolated stimulation of the diaphragm. In both cases, we stimulated the right side of the head to check if this resulted in a motor hotspot with a more distinct MEP. If this was also not possible, the subject was excluded from further TMS procedures.

The diaphragm resting motor threshold (RMT) was determined when a motor hotspot of the diaphragm was found. The RMT was defined as the lowest intensity of a single stimulus that produces a MEP with a peak-to-peak amplitude greater than 50 μV for at least 5 out of 10 stimulations.

Interstimulus intervals: Stimulations were performed to determine interstimulus interval (ISI) curves, using a paired pulse with a conditioning stimulus at 80% and a test stimulus at 125% of RMT. Fifteen stimulations were performed: five single pulses at 125% of RMT, five paired pulses with an ISI of 3 ms and five paired pulses with an ISI of 15 ms, in randomised order. During the stimulations, the subject was breathing through a mouthpiece to record the flow and pressure and MEPs were recorded in the EMG.

Recruitment curve: Lastly, the recruitment curve to TMS of the diaphragm was assessed. TMS was delivered at the end of an expiration in increments of 10% between 40% and 100% of stimulator output, with five stimuli at each level and in random order. During these stimulations, flow and mouth pressure were recorded as well.

3.3.4 Respiratory related evoked potential

During the RREP measurement, the EEG was recorded with a 128-channel system (Geodesic EEG System 400, Magstim EGI, Eugene, OR, USA). The subject breathed through a breathing system. A 128-channel EEG cap (HydroCel Geodesic Sensor Net, Magstim EGI, Eugene, OR, USA) continuously

recorded the signals of the brain. The subject breathed through the system for four blocks of approximately 10 minutes, during which inspiratory occlusions of 300 ms occurred by inflating a small balloon connected to the breathing system. The occlusions caused a complete stop of inspiratory airflow and were randomly administered after the onset of inspiration every first to fourth breath. The goal was to achieve twenty relatively artefact free occlusions for every block. Artefacts were identified by continuous visual inspection of the EEG signal, for example when the participant blinked or swallowed during an occlusion or when the trigger did not come through from the occlusion device to the EEG computer. Between every block, the impedance of the 128-channel EEG cap was checked. We aimed for an impedance of less than 100 kΩ. To mask the sound of the occlusion device, the participants were wearing noise cancelling earbuds and listened to music during the measurements. All participants were asked to keep their eyes open and to focus on one point in the room to minimise artefacts caused by alpha waves or eye movements.

3.4 Data acquisition

Physiological signals, except for EEG, were recorded through the Biopac system (MP160, Biopac Systems Inc. Goleta, CA, USA). The Biopac system was connected to AcqKnowledge software (version 5.0.2, Biopac Systems Inc. Goleta, CA, USA).

3.4.1 Hypercapnic ventilatory response curve

Flow (MP160 equipped with DA100C and TSD160E) and mouth pressure (MP160 equipped with DA100C and TSD160A) were both recorded through a sample port near the mouthpiece with a sample frequency of 2000 Hz. Near the mouthpiece were also two sample ports for PCO_2 and PO_2 (MP160 equipped with $O_2$100C and $CO_2$100C) were, that recorded with a sample frequency of 2000 Hz. EMG was recorded using surface electrodes (MP160 equipped with BIO100C and MEC110C) and with a sample frequency of 2000 Hz.

3.4.2 Transcranial magnetic stimulation

The TMS trigger was generated when one of the researchers pressed a foot pedal connected to a pressure transducer (MP160 equipped with DA100C and TSD160A), sending the trigger to the AcqKnowledge software. The TMS device received the trigger through a BNC cable, causing the device to deliver an electric pulse through the coil. For the first three subjects the sample frequency of the mouth pressure and EMG was 500 Hz. We noticed that for some stimulations, the stimulation artefact and MEP overlapped, making it difficult to isolate the MEP. For the following subjects, the sample frequency of the EMG, but also of the mouth pressure, was increased to 5000 Hz.

3.4.3 Respiratory related evoked potential

The EEG was recorded through the Geodesic EEG System 400 (Magstim EGI, Eugene, OR, USA) with a sample frequency of 250 Hz and visualised during the measurement using Net Station 5 (Magstim EGI, Eugene, OR, USA). The mouthpiece that the subject breathed through was connected to a two-way non-rebreathing valve with an inflatable balloon connected to the inspiratory port (Series 9300, Hans Rudolph Inc. Shawnee, KS, USA). Flow (MP160 equipped with DA100C and TSD160E) and mouth pressure (MP160 equipped with DA100C and TSD160A) were recorded with a sample frequency of 2000 Hz. Through the Physio16 input box (Magstim EGI, Eugene, OR, USA), the EEG system received input of the recorded mouth pressure. Inflation of the occlusion balloon and a drop in mouth pressure,

both indicating an inspiratory occlusion, resulted in two triggers that were registered in AcqKnowledge and in the EEG system. This made it possible to synchronise both systems, based on the triggers.

3.5 Data analysis

All data were analysed using MATLAB (version R2022a, MathWorks, Natick, MA, United States).

3.5.1 Hypercapnic ventilatory response curve

The HCVR provides valuable insights into the respiratory response to changes in PCO_2 levels and plays a crucial role in understanding control mechanisms of breathing. Data obtained from the measurements was pre-processed and the goal was to visualise the relationship between the increasing PCO2 and the corresponding minute ventilation.

To start the pre-processing of the data, the files were imported and the flow, O_2 and CO_2 channels were scaled. A low-pass Butterworth filter with a cutoff frequency of 10 Hz was applied to the flow signal to eliminate high-frequency noise. The Fourier transform was then utilised to compute the dominant frequency component and its corresponding cycle time, resulting in the determination of the respiratory rate and the time between two breaths. To identify the exact moment of each breath, marked at the peak of inspiration, a peak detection algorithm was used. Peaks with a minimum amplitude of 0.35 and a minimum distance of a third of the cycle time were detected. However, in some instances, the peak detection algorithm falsely identified a single breath a two separate peaks. To address this issue, a correction method was implemented where each breath was analysed to identify and correct instances of false double detections. A ‘double breath’ was characterised by the occurrence of two consecutive peaks sharing the same start and end moments of inspiration, based on the increase and decrease of the signal. To correct for the ‘double’ breath, only one of the peaks was retained.

The delay of the CO_2 and O_2 sensors compared to the flow was manually corrected by visual inspection of the flow, CO_2 and O_2 signals. The start and end points of the rebreathing phase were also manually selected based on the sudden rise and drop of the O_2 signal.

Following the pre-processing of the data, various respiratory parameters were calculated for each breath. Tidal volume was computed by summing the expiratory flow of each breath and dividing it by the corresponding breath cycle duration. Respiratory rate was determined by taking the inverse of each breath cycle duration. Minute volume, indicating the volume of air breathed in one minute, was calculated. For every respiration, the maximum $PetCO_2$ and fraction of inspired O_2 (FiO_2) were obtained. Additionally, the averages of the tidal volume and respiratory rate were calculated for the resting stage prior to the initiation of the rebreathing phase. Furthermore, $PetCO_2$ and FiO_2 levels at the end of the rebreathing phase were determined.

To visualise the relationship between $PetCO_2$ and minute ventilation during the rebreathing phase, a linear regression model was fitted to the data. In this model, $PetCO_2$ serves as the predictor, while minute ventilation is the response variable. It was assumed that VRT was reached within ten breaths from the start of the rebreathing phase. Data points above $PetCO_2$ were used to calculate the slope with a linear regression model. Model selection was based on the highest R-squared (R^2) value,

indicating better fit of the model to the data. The slope of the model was obtained, and the PAT was determined as the point where the model crossed the x-axis. The VRT, slope and PAT are shown in Figure 4 of Section 4.2.

3.5.2 Transcranial magnetic stimulation

Data analysis was performed on the short diaphragm EMG lead to obtain the peak-to-peak amplitude and the latency of the MEP. Trigger moments were identified by detecting the peaks in the derivative of a step response that indicated the occurrence of the magnetic stimulations. The trigger moments were used to segment the data into a segment of 0.25 seconds and find the location of the MEP in each segment.

The MEPs were visualised by plotting each segment. As the start and end of the MEP were difficult to detect automatically, both time points were selected manually by indicating this in the figure. These time points were used to calculate the peak-to-peak amplitude. The mean of the peak-to-peak amplitude was calculated for every condition for the ISI and recruitment curve protocols.

For the peak-to-peak amplitudes of the ISI measurements, the values of the ISI of 3 and 15 ms were expressed as a percent of the response to the single pulse. This was averaged for healthy controls and subjects with PD to produce an interstimulus response curve.

To compare the peak-to-peak amplitudes of the healthy controls with the subjects with PD, the mean values for each condition of the recruitment curve protocol were calculated for both groups and a stimulus response curve was produced.

3.5.3 Respiratory related evoked potential

EEG data segmentation was performed to isolate the EPs in each electrode. The segmentation was conducted based on the triggers corresponding to the activation of the occlusion device and the subsequent sharp drop in mouth pressure. The EPs were analysed within the segmented EEG data, focussing on the amplitude of the Nf, P1, N1, P2 and P3 components of the RREP. Pre-processing and analysis were performed using MATLAB toolboxes EEGLAB and ERPLAB [28], [29].

The pre-processing of the data involved several steps. First, EEG data were imported from Geodesic EEG system (.mff files), and the pressure signal was calibrated. Next, signals were filtered using a bandpass filter ranging from 0.5 Hz to 30 Hz and channels with various artifacts removed. These channels were interpolated using spherical interpolation, which estimates the EEG signal based on the signals from the surrounding electrode locations.

The events, containing the EPs, in the EEG data were adjusted based on the pressure trigger. Event codes were shifted in time to align with the drop in the pressure signal, indicating the start of the occlusion and the beginning of the EP. Specifically, the signal was forward shifted by 65 ms based on the pressure trigger. For two subjects, a technical issue resulted in a shorter occlusion time and therefore a slightly different pattern of the mouth pressure. For these two subjects, the signal was backward shifted with 65 ms. Subsequently, all event markers were stored in an event list.

The event markers were used to organise the EEG data into epochs and extract them from each electrode signal. The epochs were defined with start times set at 300 ms before and end times set at 1300 ms after the event marker. To enhance the signal-to-noise ratio, EEG data were re-referenced by subtracting each electrode signal from the average of all EEG electrodes, effectively removing common noise. Following this, linear trends were removed from each epoch of the EEG.

The pressure signal of each epoch was analysed to identify and eliminate epochs with false pressure triggers, thereby removing potentially unreliable EP data. Triggers were deemed suitable for further analysis only if they met the following criteria: the pressure at the epoch's onset was greater than -1 cmH_2O, the pressure in the first 50 ms transitioned from greater than -1 cmH_2O to less than -1 cmH_2O, and the pressure within the following 50 ms (from 50 ms to 100 ms) dropped to less than -2 cmH_2O. For the two subjects with the shorter occlusion time, the exclusion criteria of the pressure signal were adjusted. Only one criterium remained: the pressure in the first 200 ms from the epoch's onset decreases to less than 1.5 cmH_2O.

EP's provide accurate insights when multiple measurements are averaged. Therefore, we computed a grand average for each electrode across all subjects, both within the healthy controls and the subjects with PD. All electrodes for one RREP component were then averaged as well, based on the defined electrodes in Table 1, resulting in a group average for each RREP component. Table 1 provides an overview of the RREP components in defined brain regions with the corresponding EEG electrodes and the expected latency range, based on Von Leupoldt et al. [30]. We determined the latency and amplitude for each RREP component. The peaks seemed to have a higher latency than expected from the defined latency ranges, so we checked the signal for peaks within the latency range and the 150 ms following the range.

Table 1 Components of the respiratory related evoked potential (RREP) in defined brain regions with the corresponding EEG electrodes within the expected latency range.

RREP component	Brain region	Electrodes	Latency range (ms)
Nf	Frontal	20, 24, 28, 117, 118, 124	25-50
P1	Centro-parietal	61, 62, 78	45-65
N1	Centro-lateral	6, 7, 13, 106, 112, 129	85-125
P2	Central	6, 7, 106, 129	160-230
P3	Centro-lateral	54, 55, 61, 62, 78, 79	250-350

3.6 Statistical analysis

Statistical analyses were performed using MATLAB (version R2022a, MathWorks, Natick, MA, United States) and GraphPad Prism. For the subject characteristics and outcome parameters of the HCVR, non-parametric tests were used, as the data were not normally distributed. Data were presented as medians with interquartile ranges for continuous variables and percentages for discrete data. Differences between independent continuous variables were assessed using the Mann-Whitney-U test.

Normality was assumed for the TMS data. A repeated measures ANOVA was performed on the outcome curves of the TMS measurements. For the interstimulus curves, a one-way repeated measures was performed to examine the effect of the stimulus condition (single pulse, ISI=3 ms or ISI=15 ms) on the MEP. A two-way repeated measures ANOVA was performed on the recruitment curves. Specifically, examining the effects of the group (healthy controls or subjects with PD), the stimulator output (40% – 100%) and the interaction between group and stimulator output on the MEP.

For all statistical tests, values below $p < 0.05$ were considered statistically significant.

4. Results

4.1 Subject characteristics

A total of 9 healthy controls and 5 subjects with PD were included. Subject characteristics are presented in Table 2. Controls and subjects with PD were significantly different in age. There is no significant difference in pulmonary function between controls and subjects with PD.

Table 2 Subject demographics and pulmonary function for healthy controls (HC) and subjects with Parkinson's disease (PD)

Characteristic	HC (n=9)	PD (n=5)	p-value
Age (years)	43.0 [31.5 – 58.8]	66.0 [63.3 – 66.3]	0.02*
Sex (n male)	3 (33%)	4 (80%)	
BMI (kg/m^2)	27.4 [23.7 – 29.0]	23.9 [22.3 – 26.6]	0.20
History of smoking (n)	3 (33%)	1 (20%)	
FEV_1 (%pred)	97 [89 – 107]	110 [91 – 118]	0.30
FVC (%pred)	98 [92 – 112]	117 [103 – 123]	0.08
FEV_1/FVC	0.84 [0.71 – 0.85]	0.72 [0.70 – 0.74]	0.16
MIP (%pred)	129 [118 – 168]	103 [92 – 125]	0.11
MEP (%pred)	117 [99 – 130]	106 [86 – 117]	0.44
SNIP (%pred)	104 [90 – 129]	78 [65 – 96]**	0.05

*Discrete data are listed as n (%), continuous variables are listed as median [interquartile range]. Significant differences (p<0.05) are indicated by *. BMI: body mass index, FEV_1: forced expiratory volume in 1 second, FVC: forced vital capacity, MIP: maximal inspiratory pressure, MEP: maximal expiratory pressure, SNIP: sniff nasal inspiratory pressure.*

*** n=4, as one of the subjects with PD was not able to perform the SNIP test.*

Characteristics for every subject individually are given in Appendix B (Table 7).

4.2 Hypercapnic ventilatory response

The HCVR test was performed on 9 healthy controls and 5 subjects with PD. One subject with PD was excluded afterwards due to technical problems, which lead to the analysis of 4 subjects with PD. The threshold of 8.5 kPa that determined the end of the rebreathing phase was reached by 4 out of 9 healthy subjects and 4 out of 4 subjects with PD. The other 5 healthy controls halted the rebreathing phase early, because of discomfort.

To illustrate the test, a representative example is shown in Figure 3. Here, flow, CO_2 and O_2 for a single participant are displayed. The start of the rebreathing phase is indicated with a red dashed line and is recognisable in the O_2 signal as a sharp increase after two minutes. The is the moment the subject inhales the O2 that was added to the rebreathing bag before the test. During the rebreathing phase, the flow and CO_2 both gradually increase. The end of the rebreathing phase is indicated with a second red dashed line and is visible in the CO_2 and O_2 signals as a sharp decrease. In the following recovery phase, the flow returns to baseline.

Figure 4 shows an illustrative example of the linear regression model, based on the same participant as in Figure 3. The black line represents the linearly modelled relationship of the PetCO2 and the minute volume. The VRT is indicated as a black star. The blue points are above VRT and were used to calculate the slope. The pink points are below VRT and reflect the $PetCO_2$ where the chemoreceptors are not sensitive to changes in PCO_2. The PAT is indicated with a plus sign at the interception of the slope with the x-axis.

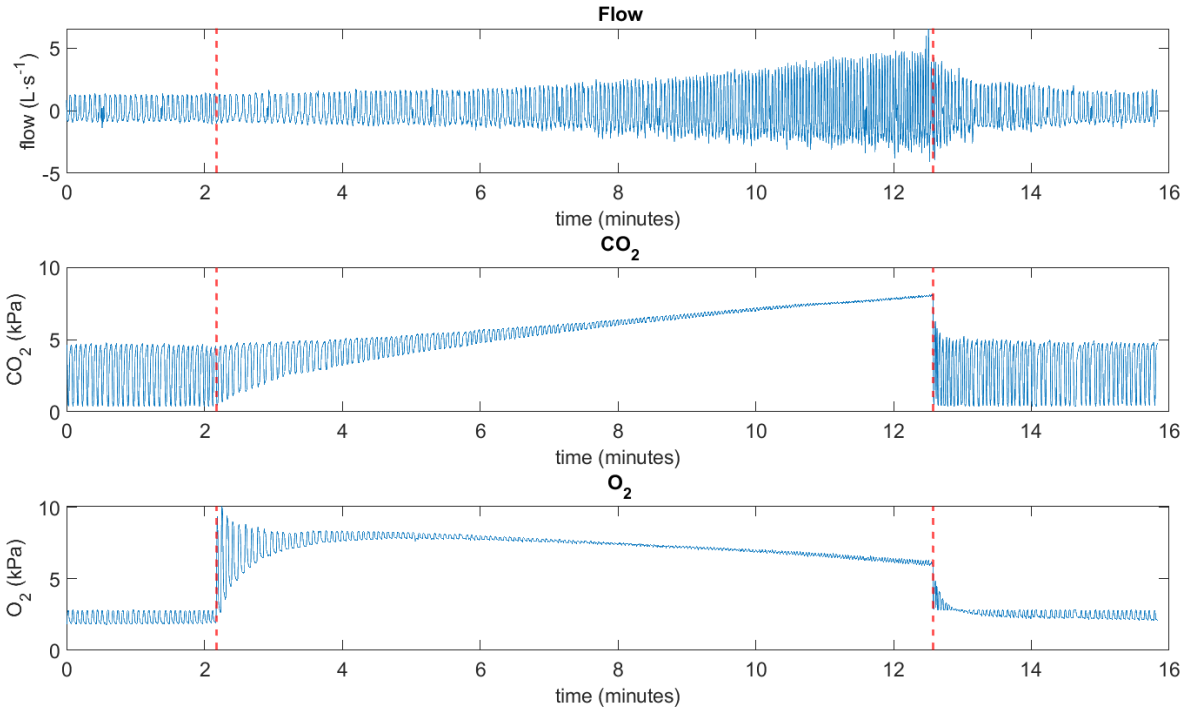

Figure 3 Hypercapnic ventilatory response for one subject. Flow, CO2 and O2 are presented. The start and end of the rebreathing phase are indicated by red dashed lines.

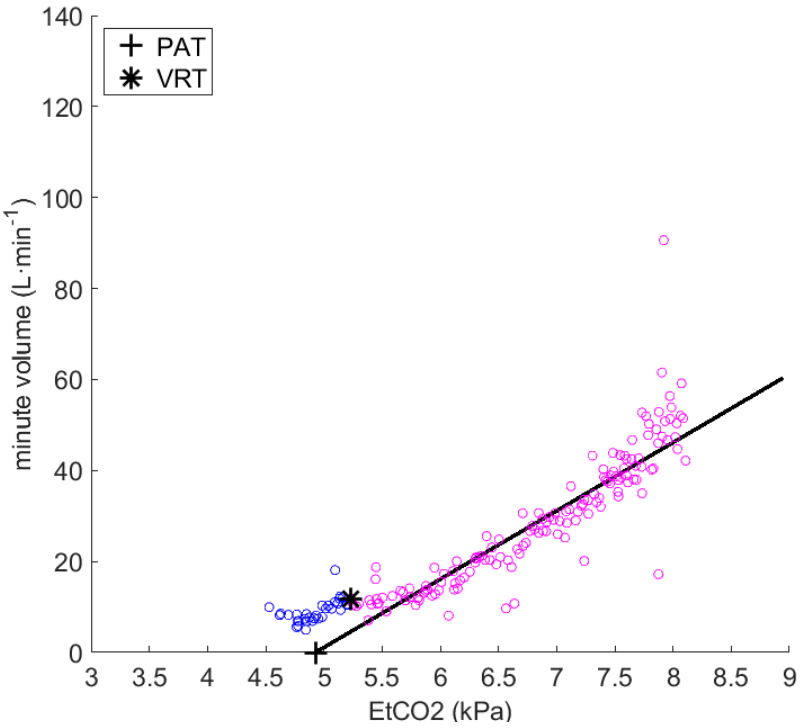

Figure 4 Linear regression model of the hypercapnic ventilatory response for one subject. The black line represents the modelled relationship between $PetCO_2$ ($EtCO_2$ on the x-axis) and minute ventilation. The projected apnoea threshold (PAT) is indicated with a plus sign and the ventilatory recruitment threshold (VRT) is indicated with a star.

The distribution of the slope of the linear regression model and PAT are displayed in Figure 5 for both groups. We found no significant difference between healthy controls and subjects with PD for slope ($p = 1.00$) and PAT ($p = 0.28$). The distributions and significance of other relevant outcomes are displayed in Table 3.

Table 3 Distribution of outcome parameters of the hypercapnic ventilatory response for healthy controls (HC) and subjects with Parkinson's disease (PD). Data are presented as median [interquartile range] with a p-value.

	HC	PD	p-value
Tidal volume at rest (ml)	685 [484 – 775]	479 [436 – 562]	0.28
Respiratory rate at rest (min^{-1})	11.9 [11.5 – 14.4]	13.5 [11.6 – 18.2]	0.15
Duration (min)	7.14 [6.51 – 8.25]	6.43 [5.86 – 6.96]	0.15

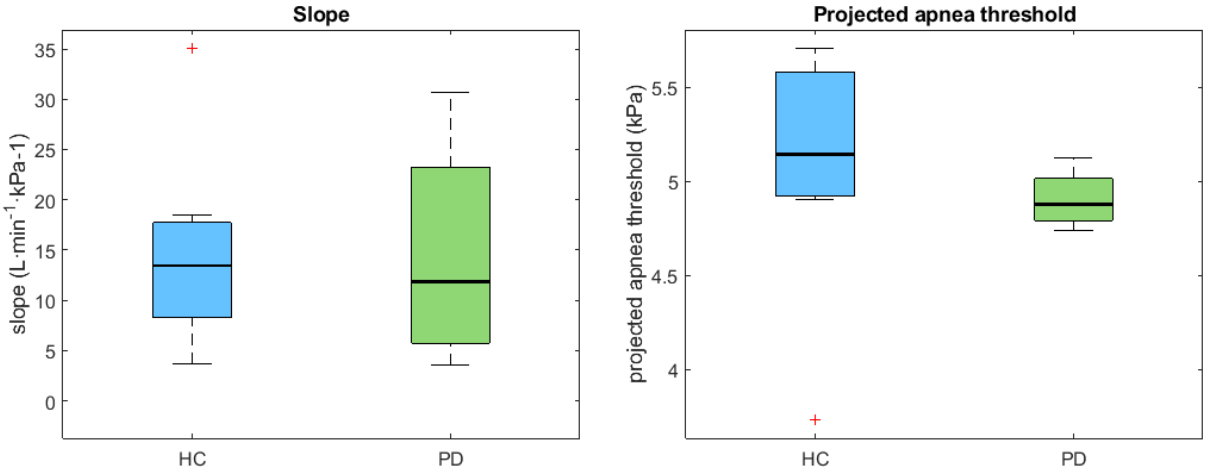

Figure 5 Boxplots of slope and projected apnoea threshold (PAT) of the hypercapnic ventilatory response for healthy controls (HC) and subjects with Parkinson's disease (PD).

4.3 Transcranial magnetic stimulation

The motor hotspot of the diaphragm was found for 6 out of 9 healthy controls and 3 out of 5 subjects with PD. The RMT for each subject is given in Table 4.

Table 4 Resting motor threshold (RMT) as a percentage of maximal stimulator output for healthy controls (HC) and subjects with Parkinson's disease (PD)

	HC1	HC2	HC3	HC5	HC7	HC9	PD3	PD4	PD5
RMT (%)	60	75	55	80	80	75	80	55	65

Interstimulus intervals: To illustrate the response to the paired pulses of TMS a representative example of a single subject is shown in Figure 6. The diaphragm MEP is displayed for the single pulse, ISI of 3 ms and ISI of 15 ms. The stimulus artefact is clearly visible for all conditions as a sharp increase and decrease of the signal. The amplitude change that follows is the MEP as recorded with the electrodes of a short diaphragm EMG lead. For this participant, the amplitude of the MEP is the greatest for the stimulation with ISI of 15 ms and the smallest for the stimulation with an ISI of 3 ms.

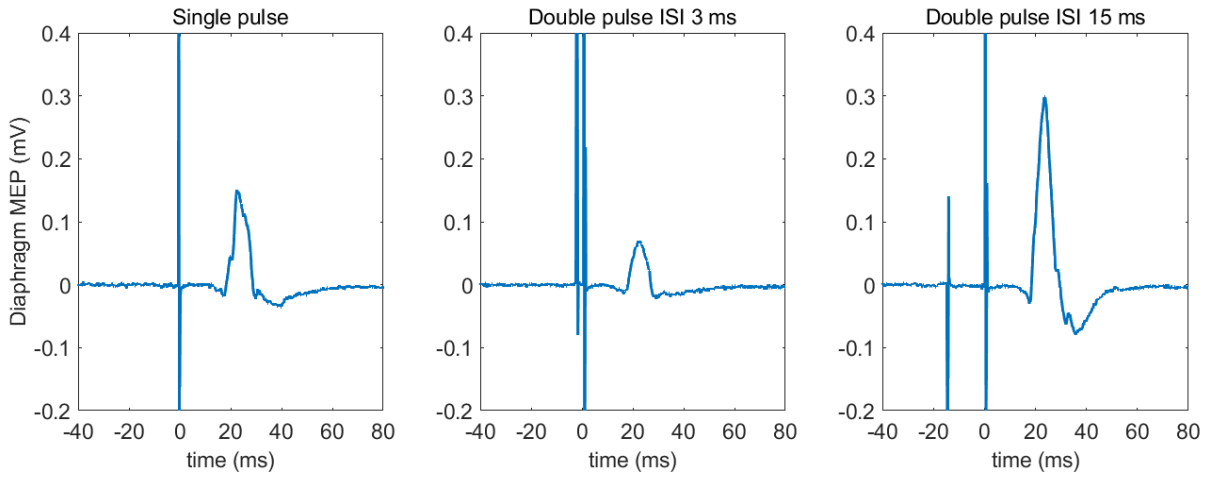

Figure 6 Motor evoked potential (MEP) of the diaphragm for three conditions: a single pulse at 125% of the resting motor threshold (RMT), a paired pulse with an interstimulus interval (ISI) of 3 ms and a paired pulse with an ISI of 15 ms. The paired pulses consist of a conditioning stimulus at 80% of RMT and a test stimulus at 125% of RMT.

Table 5 presents the absolute peak-to-peak values of the MEP for each participant for the single pulse, ISI of 3 ms and ISI of 15 ms. In Figure 7, interstimulus intervals with the peak-to-peak amplitudes of the MEP for ISI of 3 and 15 ms are visualised for healthy controls and subjects with PD. The peak-to-peak amplitudes are expressed as a percentage of the response to the single pulse stimulus. The one-way repeated measures ANOVA was performed on all participants together, without distinction between healthy controls and subjects with PD, because of the limited sample size. The ANOVA shows that there was a significant main effect of stimulus condition (single pulse, ISI=3 ms or ISI=15 ms) on the MEP ($p = 0.005$). Post hoc tests using Tukey's multiple comparisons test revealed that there was a significant difference in MEP between ISI=3 ms and ISI=15 ms ($p = 0.009$) and between single pulse and ISI=15 ms ($p = 0.038$), but not between single pulse and ISI=3 ms ($p = 0.089$).

Table 5 Peak-to-peak amplitudes of the motor evoked potential (MEP) of the diaphragm for a single pulse, a paired pulse with an interstimulus interval (ISI) of 3 ms and a paired pulse with an ISI of 15 ms. Amplitudes are presented for each subject individually.

Subject ID	Peak-to-peak amplitude single pulse (mV)	Peak-to-peak amplitude ISI=3 ms (mV)	Peak-to-peak amplitude ISI=15 ms (mV)
HC1	0.245	0.124	0.377
HC2	0.050	0.032	0.495
HC3	0.868	0.286	0.867
HC5	0.137	0.081	0.351
HC7	0.121	0.262	1.665
HC9	0.127	0.043	0.358
PD3	0.624	0.444	2.502
PD4	0.545	0.205	1.354
PD5	1.251	0.801	1.988

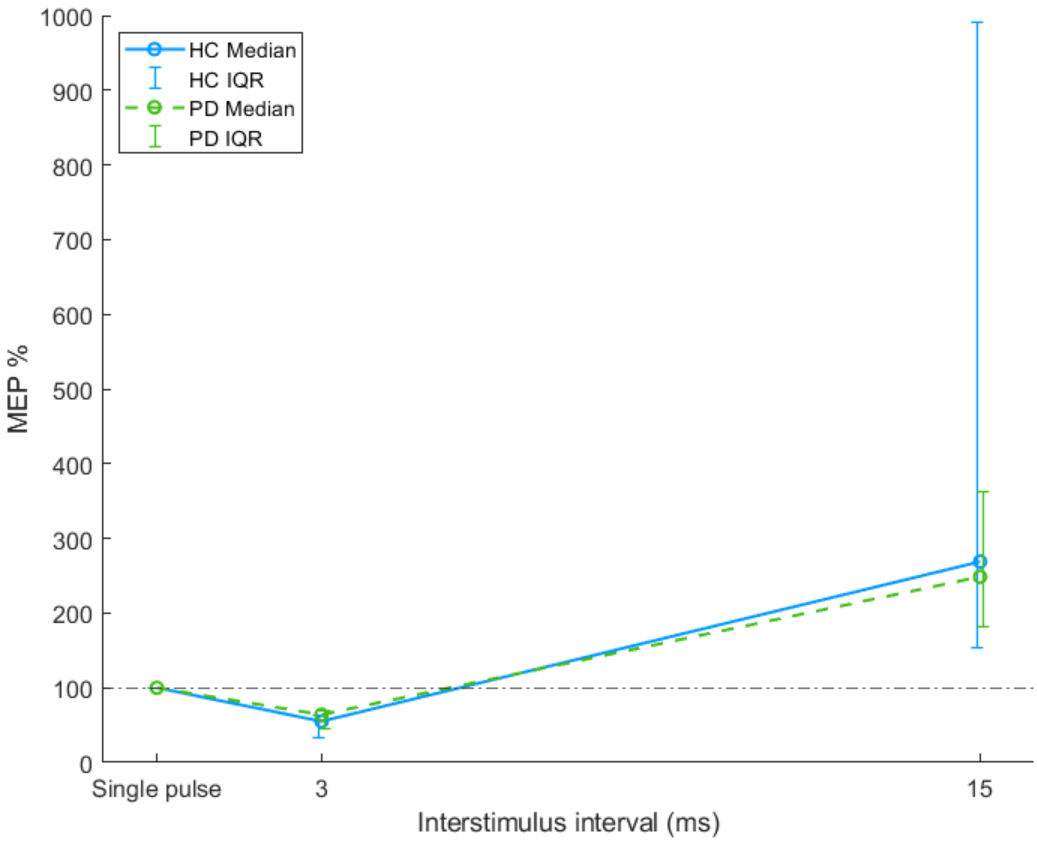

Figure 7 Interstimulus response curve of the motor evoked potential (MEP) for healthy controls (HC) and subjects with Parkinson's disease (PD). Data points are presented as the median with error bars for the interquartile range.

Recruitment curve: In Figure 8, a representative example of the response to increasing TMS stimulus is shown. The diaphragm MEP for a single subject is plotted for the recruitment curve at 40% to 100% of stimulator output. The amplitude of the MEP increases as the stimulator output increases.

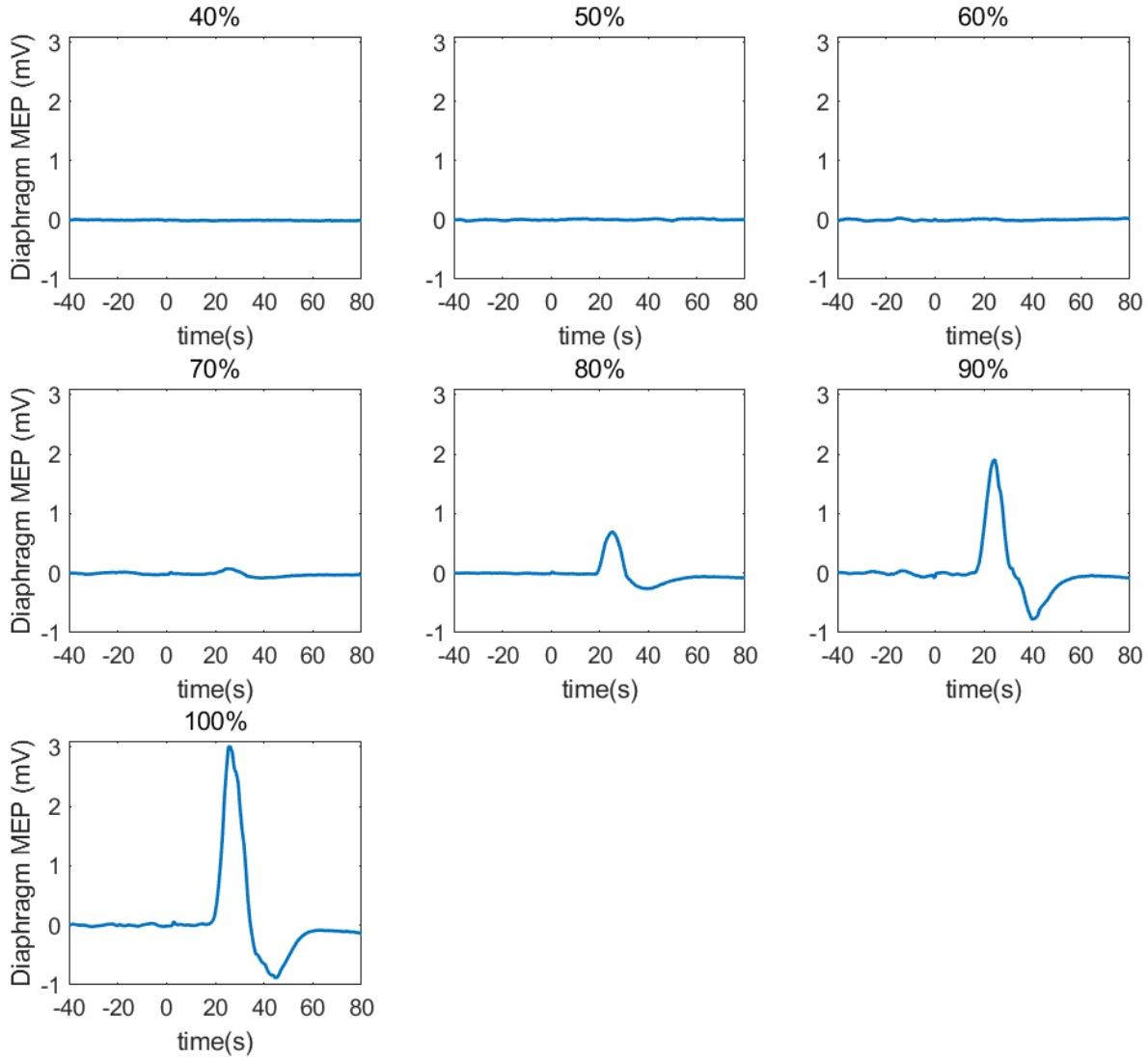

Figure 8 Representative example of the motor evoked potential (MEP) of the diaphragm for stimuli ranging from 40% to 100% of stimulator output.

Table 6, the mean peak-to-peak amplitude of the MEP of the diaphragm is presented for each subject individually. In Figure 9, the recruitment curves are visualised for healthy controls and subjects with PD. The MEP amplitudes for subjects with PD show an increase from baseline at 50%, whilst the MEP amplitudes for healthy controls increase at 70%. The two-way repeated measures ANOVA shows no significant main effect on the MEP of group (healthy controls or subjects with PD) ($p = 0.493$) or stimulator output (40% – 100%) ($p = 0.059$). There was also no significant effect of the interaction between group and stimulator output ($p = 0.982$).

Table 6 Peak-to-peak amplitude of the motor evoked potential (MEP) of the diaphragm for increasing stimulator output, presented as a percentage of maximal stimulator output. Amplitudes are presented for each subject individually.

Subject ID	MEP at 40%	MEP at 50%	MEP at 60%	MEP at 70%	MEP at 80%	MEP at 90%	MEP at 100%
HC1	0.004	0.005	0.019	0.109	0.189	0.365	0.674
HC2	0.005	0.010	0.013	0.025	0.059	0.094	0.273
HC3	0.010	0.027	0.043	0.324	1.287	2.851	3.206
HC5	0.005	0.005	0.004	0.015	0.031	0.072	0.115
HC7	0.016	0.013	0.009	0.036	0.044	0.059	0.113
HC9	0.007	0.006	0.024	0.141	0.176	0.300	0.487
PD3	0.023	0.024	0.044	0.092	0.181	0.401	0.503
PD4	0.007	0.018	0.290	0.799	0.785	1.571	1.995
PD5	0.016	0.037	0.266	0.529	0.575	0.773	0.857

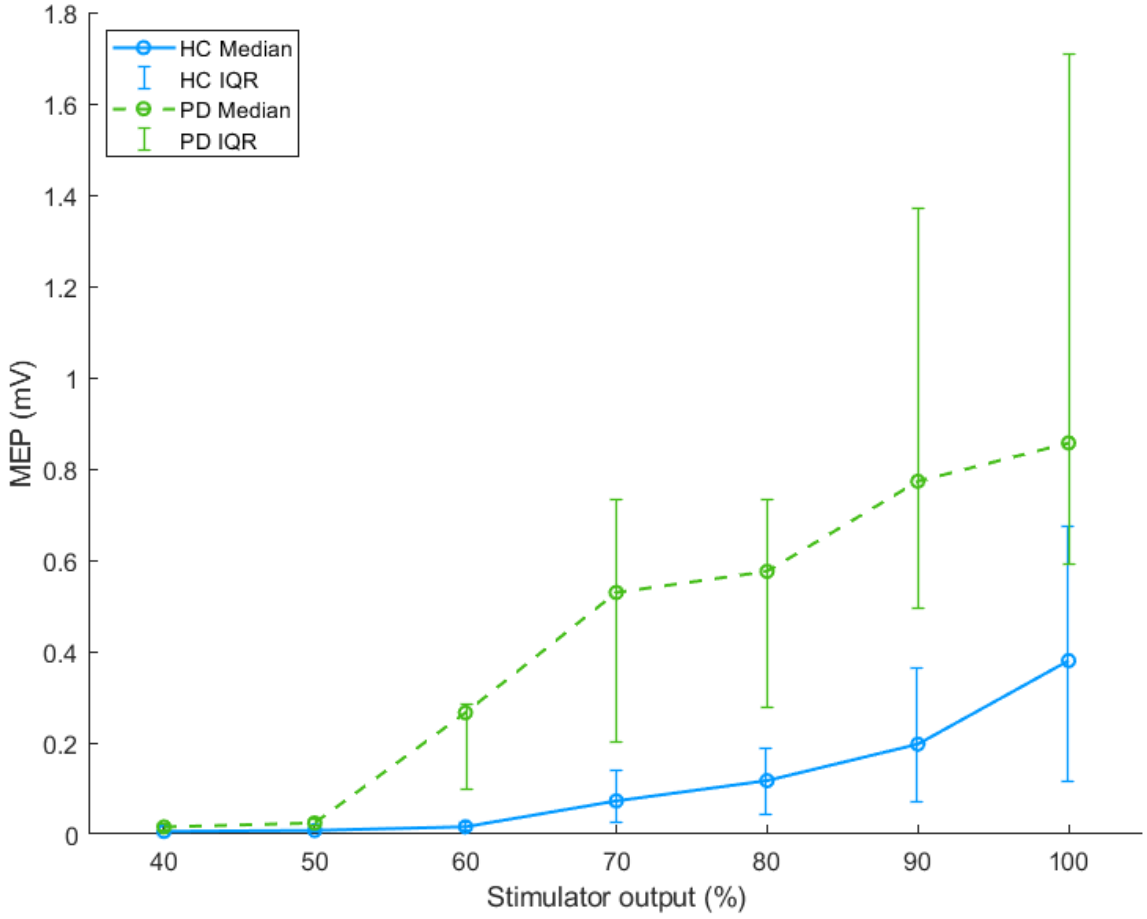

Figure 9 Recruitment curves with peak-to-peak amplitudes of the motor evoked potential (MEP) of the diaphragm for increasing stimulator output. Healthy controls (HC) are plotted as a solid blue line with markers at the median MEP, subjects with Parkinson's disease (PD) are plotted as a dashed green line.

4.4 Respiratory related evoked potentials

RREP measurements were performed on all 14 participants. In Figure 10, the group average is visualised for each RREP component for the healthy controls and subjects with PD. The locations of the RREP components are indicated with red circles. The latency and amplitude for each RREP component are presented in Appendix B (Table 9).

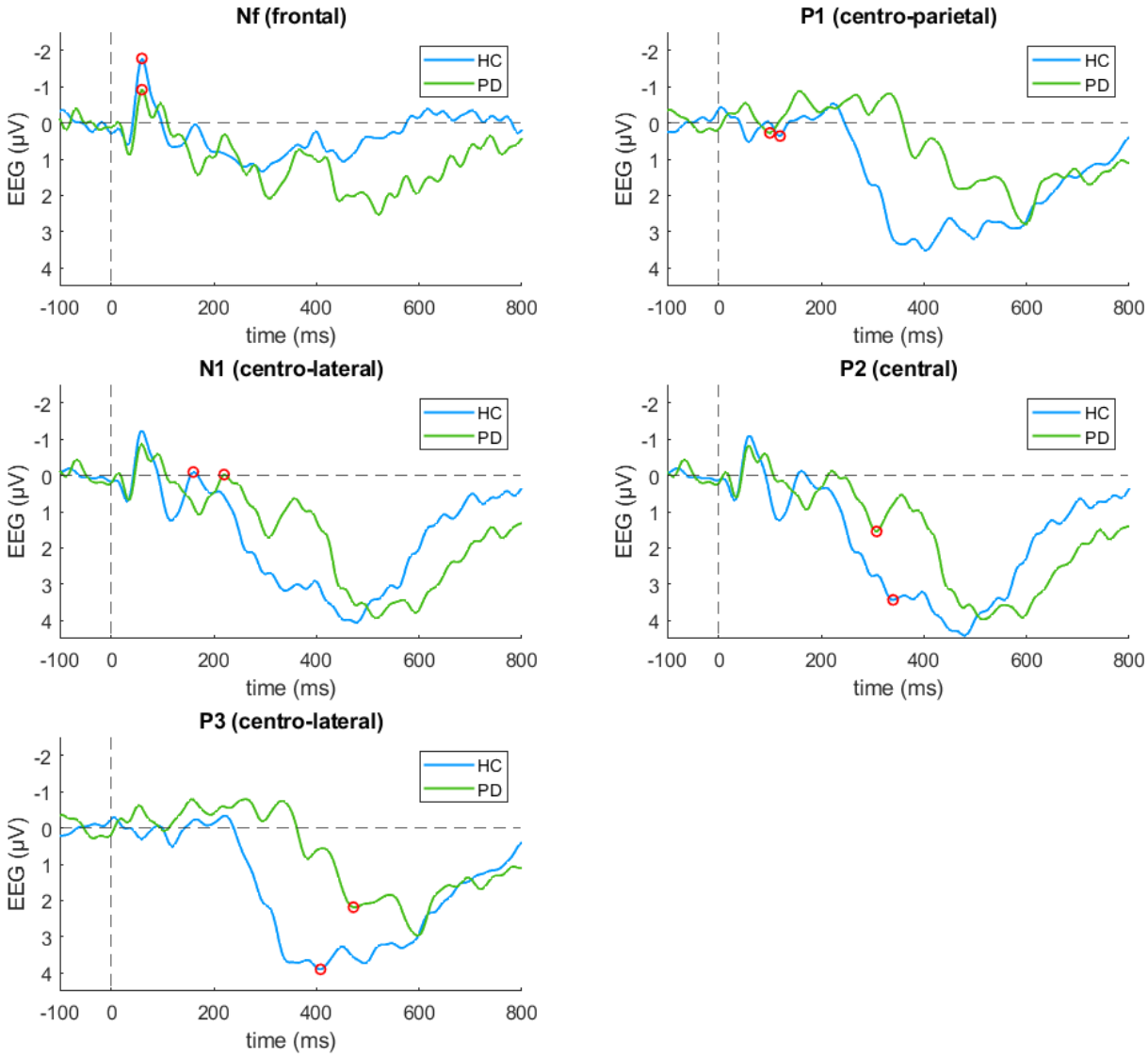

Figure 10 Group average of the respiratory related evoked potentials (RREP) for all components for the healthy controls (HC) and subjects with Parkinson's disease (PD). At t = 0 ms, the mouth pressure drops, which induces the RREP. The components are indicated with a red circle.

For the N1 and P3, the RREP arrives later for the subjects with PD than for the healthy controls. Moreover, the magnitudes of the amplitude of all RREP components are lower for the subjects with PD compared to healthy controls.

Scalp topography plots are visualised for both groups in Figure 11. For each scalp plot, the latency of the RREP component is taken as time point.

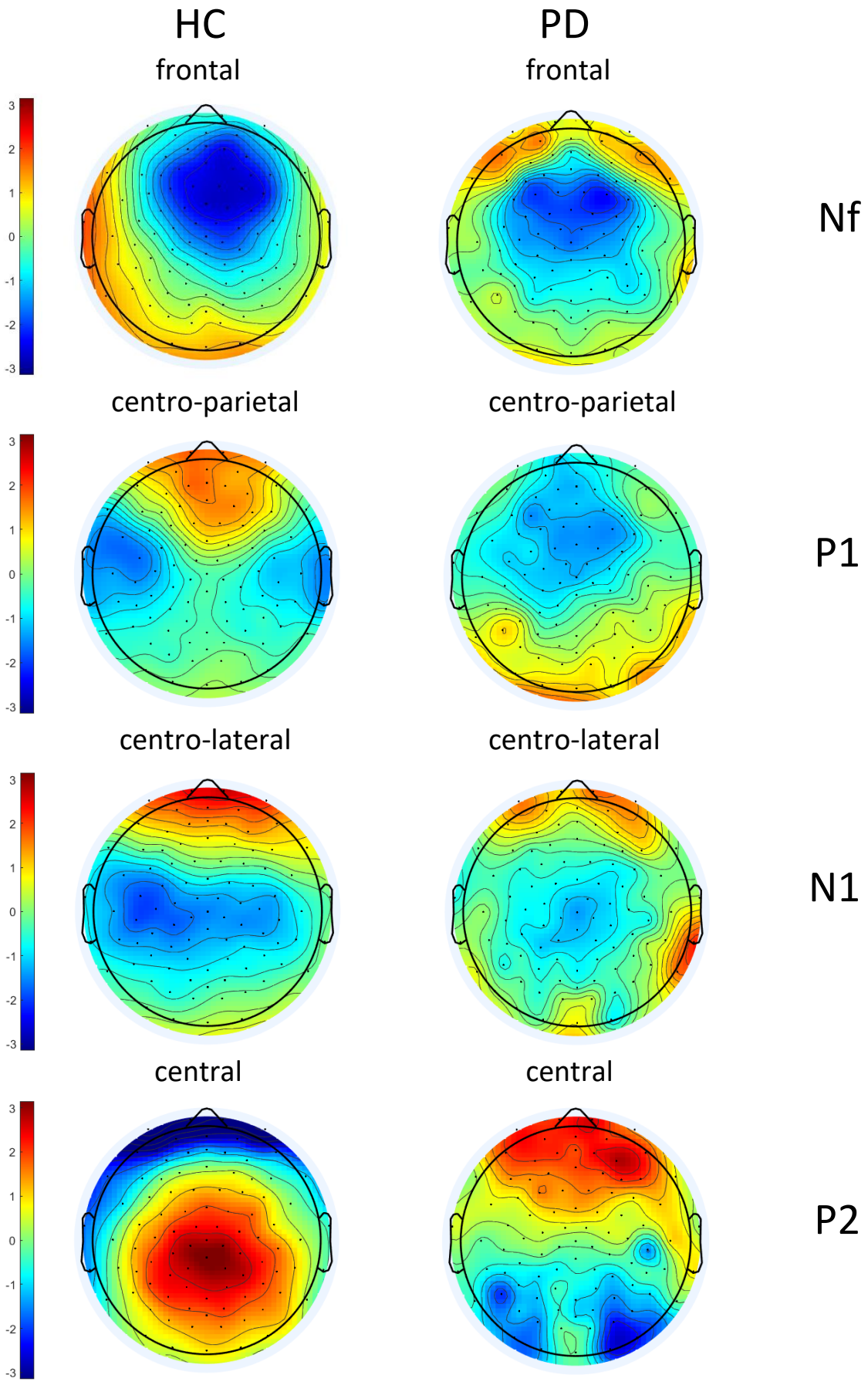
HC
PD
frontal
frontal
Nf
centro-parietal
centro-parietal
P1
centro-lateral
centro-lateral
N1
central
central
P2
3
2
1
0
-1
-2
-3

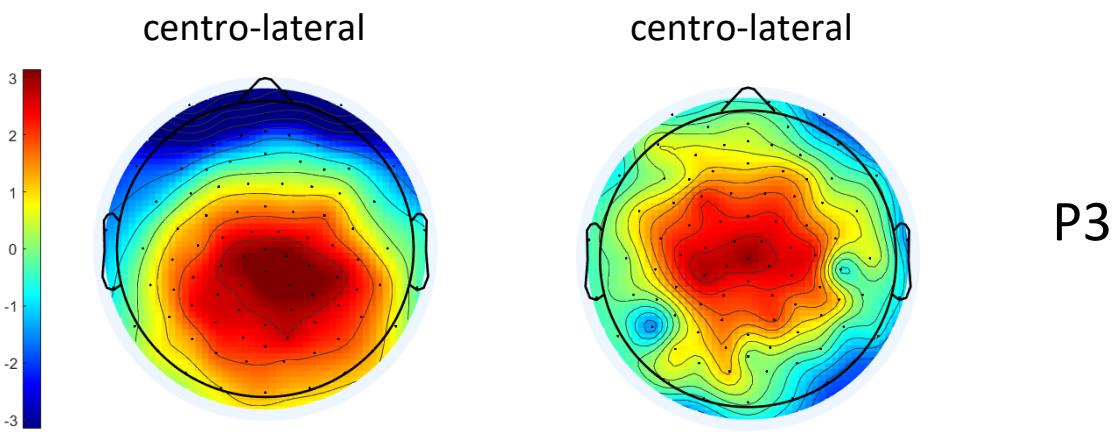

Figure 11 Scalp topography plots of all RREP components for heathy controls (HC) and subjects with Parkinson's disease (PD) with the corresponding brain region. For each plot, the latency of the corresponding RREP component for that group is taken as time point, equivalent to the red circles in Figure 10.

The Nf and the P3 components are clearly visible in the scalp topographies for both healthy controls and subjects with PD. Both components exhibit a higher magnitude and a larger distribution over the corresponding brain region. The P1 component is not clearly visible in the scalp topography for either group. For healthy controls, the N1 component is more pronounced on the left side. The P2 component is clearly visible at the central region of the brain for healthy controls, but not for the subjects with PD. For these subjects, the scalp plot of P2 shows a positive signal in the frontal region, and a negative signal appears bilaterally in the temporal region.

5. Discussion

This study aimed to investigate whether neural control of breathing is impaired in PD using advanced neurophysiological techniques. Our preliminary findings indicate that there are differences in neural control of breathing for subjects with mild to moderate PD on dopaminergic medication, compared to healthy controls. Specifically, data from TMS revealed increased cortical excitability of the motor pathways to the diaphragm for subjects with PD. We found attenuated first-order and cognitive processing in the perception of respiratory sensations in subjects with PD. We found no differences in chemosensitivity to PCO_2 between groups, suggesting an intact response of minute ventilation to PCO_2. While these results are preliminary, they provide a valuable insight that neural control of breathing may be impaired in individuals with mild to moderate PD on dopaminergic medication.

Given the inclusion of 9 healthy controls and 5 subjects with PD, the sample size is limited. The primary focus in this discussion will be on the observed trends in the results, rather than solely relying on statistical significance.

5.1 Pulmonary function

As expected, pulmonary function was not statistically different between healthy controls and subjects with PD. However, the FEV_1/FVC ratio for PD is close to the threshold that is used for diagnosing chronic pulmonary obstructive disease (COPD). This could suggest that the individuals with PD lean towards a more obstructive pulmonary function, which is a common symptom in PD [12], [31]. The FEV_1/FVC ratio does also decline with age, so this could also be an explanation for the lower values, as the subjects with PD were significantly older [32].

The SNIP test shows notable differences between the two groups, even though these are not significantly different. This can be attributed to the complexity of the performance of the test. Subjects frequently encountered challenges in following the instructions, particularly those with PD who struggled with managing multiple instructions simultaneously. This difficulty may have contributed to the lower values observed in this group.

5.2 Hypercapnic ventilatory response

There is not much data available on the hypercapnic response when using a rebreathing test. This makes it difficult to assess whether our results fall within the normal values. One study has assessed two different techniques of the HCVR, including the rebreathing test [22]. In general, our values of the slope and PAT seem to be in line with this study.

At rest, subjects with PD have a higher respiratory rate with a lower tidal volume compared to healthy controls. Tachypnoea is a known phenomenon in PD and can also be a side effect of levodopa on breathing [12].

There is no difference in slope between healthy controls and subjects with PD, implying that a change in PetCO2 does not result in a different response for both groups. This means that we found no change in chemosensitivity for PCO_2 for individuals with mild to moderate PD on dopaminergic medication. This finding is supported by other studies, where an unchanged response to hypercapnia is mainly seen in mild to moderate stages of PD as well [12], [33]. A difference in chemosensitivity of the $PetCO_2$

and minute ventilation is found in subjects with a more advanced Hoehn and Yahr stage than the subjects in this study [12], but this is not reflected in our findings, as we only included subjects with mild to moderate disease stage. It is important to note, however, that these previous studies used different techniques of obtaining the HCVR, which might lead to different results.

The duration of the rebreathing phase is lower for the subjects with PD. The cause of this is unclear, but it might be related to their higher respiratory rate at rest, possibly shortening the time to reach the PCO_2 threshold. The PAT is the interception of the slope of the HCVR with the x-axis and is the level of PCO_2 were, hypothetically, ventilation ceases [22]. The results show that the PAT is slightly lower for the subjects with PD compared to the controls. A lower PAT would suggest that for individuals with PD ventilation ceases for a lower PCO_2. This means that they would already hypothetically stop breathing at a lower level of PCO_2. Although there seems to be a slight difference in PAT between groups, we do not view this difference as substantial enough to conclude that the HCVR has changed for subjects with PD.

5.3 Transcranial magnetic stimulation

The response to TMS on the motor hotspot of the diaphragm was compared in subjects with PD and healthy controls. The goal was to compare cortical excitability of the motor pathways to the diaphragm, testing the hypothesis that individuals with PD might have a higher cortical excitability of the diaphragm and are therefore more easily stimulated.

The motor hotspot of the diaphragm was not found for every subject. Some of the subjects showed little response to the magnetic pulse, which lead to the exclusion of these subjects. It is unclear why this happened for such a large proportion of the subjects. The protocol of this study was based on a study by Chakalov et al. and the same devices were used [14]. Interestingly, they found the motor hotspot of the diaphragm in all twenty of their subjects, whereas we only found it in nine out of fourteen subjects. The main difference between the two studies was the age of the subjects. Chakalov et al. only stimulated subjects between the age of 19 and 38. This could cause the difference in the number of subjects that we found the motor hotspot for, as the age of our subjects ranged from 24 to 67. Bhandari et al. studied the effect of aging on the motor cortex neurophysiology assessed by TMS and found that cortical excitability is dependent on age [34]. RMT increased significantly with age, which may be contributed to CNS decline and anatomical and functional integrity changes of the brain. An increase in RMT may result in a motor hotspot that is difficult to find, because the stimulator output may not be high enough to elicit enough response. In our study, the motor hotspot was not found for healthy subjects of ages 32, 43 and 61 years old. The motor hotspot was also not found for one subject with PD with an age of 61 years old. Considering the increase of RMT with age, this may be one of the reasons that we did not find the motor hotspot for three healthy subjects.

Interstimulus intervals: At an ISI of 3 ms, we would expect to see inhibition, mediated by GABA-A receptors [35]. At an ISI of 15 ms, the effect is facilitatory, which is thought to be caused by the activation of cortico-cortical pyramidal cells and their excitatory glutaminergic synapses [36]. The inhibitory and facilitatory effects are visible in this present study for both groups. The significant differences between single pulse and an ISI of 15 ms and the difference between an ISI of 3 ms and 15 ms show that the expected inhibitory and facilitatory effects of the paired stimuli are present. This means that the excitability of the intracortical inhibitory and excitatory circuits are as expected and

confirms that our method of TMS was correct. The ISI response curve does not differ between subjects with PD and healthy controls. This suggests that there is no substantial difference between the groups in terms of the excitability of the intracortical inhibitory and excitatory circuits.

Recruitment curve: The recruitment curves are not significantly different between groups, as tested with the two-way repeated measures ANOVA. Nonetheless, a trend can be observed when visually inspecting the curves. For subjects with PD, the response starts at an earlier stimulator output and reaches a higher MEP at 100% of stimulator output than for healthy controls. Both results may lead to increased cortical excitability of the diaphragm for subjects with PD. Moreover, the curve for healthy controls keeps steadily increasing until 100% of stimulator output, whereas the curve for subjects with PD seems to reach a plateau when it nears 100% of stimulator output. This flattening might suggest that the subjects with PD reach the maximum activation of their diaphragm at a lower stimulus. This means that they may have less reserve of their diaphragm and may not be able to increase its activity enough when necessary, leading to inadequate ventilation. Although the groups are different in age, we hypothesise that this is not the reason for the difference in cortical excitability of the diaphragm between groups, as cortical excitability usually decreases with healthy aging [34].

The increased cortical excitability in subjects with PD is also found in other studies [37]. Larger MEPs are found in other muscles, suggesting higher cortical excitability in general. It is, however, unclear what the effect is of dopaminergic medication.

Hopkinson et al. compared cortical excitability of the diaphragm between individuals with COPD and healthy controls [36]. Interestingly, they found similar results for the recruitment curves of individuals with COPD. The lack of reserve of the diaphragm, resulting from the flattening recruitment curve, is similarly identified in subjects with COPD. They hypothesise that this plateau of the recruitment curve may make COPD patients more vulnerable to increases in load during acute exacerbations.

5.4 Respiratory related evoked potential

The RREP to a short inspiratory occlusion in subjects with PD was compared to healthy controls. The goal was to evaluate how the brain processes respiratory input signals and we hypothesised that in subjects with PD, the RREP components would be less frequently present or reduced in amplitude.

All peaks have a higher latency than expected from earlier studies [15], [30]. This could be caused by methodological differences between our study and previous studies. The main difference was the use of an inflatable balloon for inflation instead of an occlusion valve. Both methods make it possible to occlude the inspiratory port and can control the occlusion time. However, earlier studies have found that there is a slight delay when using the balloon compared to the valve. In our analysis, we compensated for this difference by defining the onset of the occlusion at the moment the mouth pressure begins to drop and not at the time of the occlusion trigger. This still resulted in longer latencies, so there might be a difference in physiological response as well as a difference in delay when using our method. The occlusion time is also different compared to some studies, but Webster et al. compared different occlusion durations and did not find a difference in either amplitude or latency of the RREP [38]. It is unlikely that this is the cause of the difference in latencies in the current study.

The amplitude of all RREP components is lower in magnitude for the subjects with PD compared to healthy controls. There does not seem to be a difference in earlier (Nf, P1, N1) and later (P2, P3) components. This suggests that there is an attenuated first-order and cognitive processing in subjects with PD compared to healthy controls. The amplitudes of P2 and P3 are related to the sensation of respiratory stimuli [25], [26]. The findings could imply a decreased capacity to detect changes in respiratory mechanics and therefore a declined perception of respiratory sensations in subjects with PD.

Amplitude of certain peaks is influenced by the subject's attention to the inspiratory occlusion. Previous studies have found a decrease in amplitude for N1, P2 and P3 when a subject was not attentive to the occlusions [30], [39]. In our study, we neither instructed the subjects to focus on the occlusion nor distracted them. However, we observed that the subjects with PD had more difficulty staying awake during the RREP measurements compared to the healthy controls, thus being less attentive to the occlusions. This could potentially attribute to the lower amplitude observed for N1, P2 and P3 in subjects with PD.

The latency of the peaks for nearly all RREP components is higher for subjects with PD. Epiu et al. studied the effect of age on the latency of the RREP and found that there was a higher latency in the group with a mean age of 76 years old compared to the group with a mean age of 30 years old [40]. The increased latency shows a delayed neural response to airway occlusion, suggesting that there is impaired processing of sensory inputs in healthy aging. In our current study, the age difference between the healthy controls and the subjects with PD may contribute to the difference in latencies across the groups.

For some RREP components it was difficult to identify the correct peaks. We used a peak detection algorithm to detect peaks within the defined range but relied on visual identification to select the right peak. The exact delay of our signals remains unclear, which complicates determining which peak was the right representation of the RREP component. Upon examining the scalp topographies, we notice that some peaks are difficult to distinguish. For P1, this is most likely due to the small magnitude. Additionally, the question is raised of whether the previously recommended locations of the electrodes were optimal for each RREP component, for example for N1, where the activity seems to be even more lateral than our chosen electrodes [30]. There is also activity visible in the scalp plots that we cannot explain, for example the positive frontal signal in the scalp plot for component P2 for the subjects with PD. It remains unclear whether this might be caused by noise or a potential physiological component in PD and if P2, among other peaks, was selected correctly.

5.5 Integration of the findings

When considering the pathway of neural control of breathing, all tests measure different components of the entire pathway. Although the measurements provide interesting results individually, the complete pathway of neural control of breathing in subjects with PD can only be evaluated when all measurements are integrated. Integrating all measurements is challenging and there is not one single correct approach to do this. To make this easier, the simplified scheme of neural control of breathing (as depicted in Figure 1) will be used as a reference.

The HCVR measures the chemosensitivity to PCO_2 as indicated in Figure 12 of Appendix A. The HCVR showed no convincing differences between subjects with PD and healthy controls. Therefore, we assume that the functionality of the pathway measuring chemosensitivity to PCO_2 is unchanged in individuals with mild to moderate PD on dopaminergic medication.

TMS targets the motor cortex and its results are measured directly at the receiving muscle, the diaphragm (Appendix A, Figure 13). This mainly captures the motor pathway from the brain to the respiratory muscles. The observed increase in cortical excitability suggests an impaired motor pathway from the brain to the respiratory muscles in PD.

The RREP on the other hand, starts at the expansion of the chest wall and the lungs (Appendix A, Figure 14). Its resulting signal is measured at the somatosensory cortex, thereby capturing the sensory pathway of neural control of breathing from the respiratory muscles to the brain. The results of the RREP in subjects with PD indicate that there is an impaired pathway from the respiratory muscles to the brain. Subjects with PD seem to have a lower capacity to detect changes in respiratory sensations. They might not adequately sense respiratory changes, such as dyspnoea, which could potentially make it challenging for them to adjust their breathing response to these modified sensations.

An unchanged HCVR combined with an impaired response to TMS and an attenuated RREP, suggests that the chemosensitivity to PCO_2 seems in order, but there seem to be changes in the motor pathway and the sensory pathway of breathing. This would suggest that neural control of breathing is impaired in individuals with mild to moderate PD on dopaminergic medication.

5.4 Limitations

The study was conducted with a limited number of participants, making the results and their interpretation preliminary. The ultimate objective of the study is to have fifteen participants in each group. However, this was not achieved by the time this report was finished. Therefore, whilst the initial findings provide some insights, they may not be entirely representative of the results that could be obtained with a larger sample size. A continuation of this research with more participants is necessary to validate these preliminary findings.

Patients were asked to continue their dopaminergic medication on the day of the measurement. This ensured that they were not too influenced by their symptoms and thus were able to tolerate the tests better than if they had to stop their medication. Another reason for asking the patients to continue their medication was so that we could measure control of breathing in their everyday condition. A limitation of the medication use was that we do not know if the observed responses are purely caused by alterations in disease, or if their dopaminergic medication had an effect as well. Earlier studies of TMS of muscles of the hand in subjects with PD, found an altered response even when medication was continued, which could mean that this would be the case in our study as well when subjects had not continued their medication [41].

We assume that the contraction of respiratory muscles is not affected by the motor symptoms, because we only included patients with mild to moderate disease stages. This would imply that our results are not caused by motor symptoms of PD. However, there might still be some muscle weakness

or rigidity of the respiratory muscles present in subjects with PD, as this is not always immediately reflected in pulmonary function.

It was difficult to distinguish the response of the diaphragm and other respiratory muscles during TMS. We do therefore not know if co-activations of muscles other than the diaphragm are presented in the results as well. The calculated MEPs might be higher than the MEP of the diaphragm alone would have been, because of activation of the nearby muscles. The TMS coil that was used in this study has a very focal field, meaning that a small part of the motor cortex was stimulated. But some activity was still seen in other respiratory muscles and the waveform of the MEP for some stimulations was different than the expected biphasic response that we saw during electrical stimulation of the phrenic nerve.

For the RREP, a high-density EEG cap was used. This cap used conductive (salted) water instead of the usual gel. A lot of locations of the brain were measured in a relatively short amount of preparation time, but this also caused relatively high impedances. This led to a higher signal-to-noise ratio. This was tackled by using more occlusion for averaging of the signal [30].

6. Conclusion

This study provides new insights into the neural control of breathing in PD. Using advanced neurophysiological techniques, we observed increased cortical excitability of the motor pathways to the diaphragm with TMS and attenuated processing of respiratory signals with RREP measurements for subjects with PD compared to healthy controls. Interestingly, chemosensitivity to PCO_2, measured with HCVR, appears to remain unaffected in our subjects with PD. These findings collectively indicate that both the sensory and motor pathways involved in neural control of breathing are impaired in individuals with mild to moderate PD on dopaminergic medication, whilst chemosensitivity to PCO_2 remains intact. This is a significant step forward in our understanding of this disease. Whilst further research is still necessary, a better understanding of neural control of breathing in PD can ultimately lead to new treatments of respiratory dysfunction.

References

[1] M. J. A. M. van Putten, *Essentials of neurophysiology: basic concepts and clinical applications for scientists and engineers*. Springer, 2009.

[2] M. J. T. Fitzgerald, E. Mtui, G. Gruener, and P. Dockery, *Fitzgerald's clinical neuroanatomy and neuroscience*, 7th ed. Elsevier Inc, 2016.

[3] S. Vijayan, B. Singh, S. Ghosh, R. Stell, and F. L. Mastaglia, "Brainstem ventilatory dysfunction: A plausible mechanism for dyspnea in Parkinson's Disease?," *Movement Disorders*, vol. 35, no. 3, pp. 379–388, 2020.

[4] R. B. dos Santos *et al.*, "Respiratory muscle strength and lung function in the stages of Parkinson's disease," *Jornal Brasileiro de Pneumologia*, vol. 45, 2019.

[5] E. M. Guilherme, R. de F. C. Moreira, A. de Oliveira, A. M. Ferro, V. A. P. Di Lorenzo, and A. C. L. Gianlorenco, "Respiratory disorders in Parkinson's disease," *J Parkinsons Dis*, vol. 11, no. 3, pp. 993–1010, 2021.

[6] H. H. Fernandez and K. L. Lapane, "Predictors of mortality among nursing home residents with a diagnosis of Parkinson'sdisease.," *Medical Science Monitor*, vol. 8, no. 4, pp. CR241–CR246, 2002.

[7] A. O'Callaghan and R. Walker, "A review of pulmonary function in Parkinson's disease," *Journal of Parkinsonism and Restless Legs Syndrome*, 2018.

[8] A. D'Arrigo *et al.*, "Respiratory dysfunction in Parkinson's disease: a narrative review," *ERJ Open Res*, vol. 6, no. 4, 2020.

[9] M. Pokusa, D. Hajduchova, T. Buday, and A. K. Trancikova, "Respiratory function and dysfunction in Parkinson-type neurodegeneration," *Physiol Res*, vol. 69, no. Suppl 1, p. S69, 2020.

[10] L. McMahon, C. Blake, and O. Lennon, "A systematic review and meta-analysis of respiratory dysfunction in Parkinson's disease," *Eur J Neurol*, vol. 30, no. 5, pp. 1481–1504, 2023.

[11] W. Zhang *et al.*, "Dysregulation of respiratory center drive (P0. 1) and muscle strength in patients with early stage idiopathic Parkinson's disease," *Front Neurol*, vol. 10, p. 724, 2019.

[12] K. Kaczyńska, M. E. Orłowska, and K. Andrzejewski, "Respiratory Abnormalities in Parkinson's Disease: What Do We Know from Studies in Humans and Animal Models?," *Int J Mol Sci*, vol. 23, no. 7, p. 3499, 2022.

[13] T. Vassilakopoulos, "Chapter 6 - Control of Ventilation and Respiratory Muscles," S. G. Spiro, G. A. Silvestri, and A. B. T.-C. R. M. (Fourth E. Agustí, Eds., Philadelphia: W.B. Saunders, 2012, pp. 50–62. doi: https://doi.org/10.1016/B978-1-4557-0792-8.00006-4.

[14] I. Chakalov *et al.*, "The role of the TMS parameters for activation of the corticospinal pathway to the diaphragm," *Clinical Neurophysiology*, vol. 138, pp. 173–185, 2022.

[15] P.-Y. S. Chan and P. W. Davenport, "Respiratory related evoked potential measures of cerebral cortical respiratory information processing," *Biol Psychol*, vol. 84, no. 1, pp. 4–12, 2010.

[16] J.-P. Lefaucheur, “Motor cortex dysfunction revealed by cortical excitability studies in Parkinson’s disease: influence of antiparkinsonian treatment and cortical stimulation,” *Clinical Neurophysiology*, vol. 116, no. 2, pp. 244–253, 2005.

[17] R. Cantello, R. Tarletti, and C. Civardi, “Transcranial magnetic stimulation and Parkinson’s disease,” *Brain Res Rev*, vol. 38, no. 3, pp. 309–327, 2002.

[18] B. Fauroux *et al.*, “Impaired cortical processing of inspiratory loads in children with chronic respiratory defects,” *Respir Res*, vol. 8, no. 1, pp. 1–8, 2007.

[19] W. F. Boron and E. L. Boulpaep, “The Respiratory System,” in *Medical physiology*, Updated 2n., Elsevier Inc, 2012.

[20] R. M. Schwartzstein and M. J. Parker, *Respiratory physiology: a clinical approach*. Lippincott Williams & Wilkins, 2006.

[21] D. W. Dickson, “Neuropathology of Parkinson disease,” *Parkinsonism Relat Disord*, vol. 46, pp. S30–S33, 2018.

[22] D. C. Mannée, T. M. Fabius, M. Wagenaar, M. M. M. Eijsvogel, and F. H. C. de Jongh, “Reproducibility of hypercapnic ventilatory response measurements with steady-state and rebreathing methods,” *ERJ Open Res*, vol. 4, no. 1, 2018.

[23] J. Valls-Solé, A. Pascual-Leone, J. P. Brasil-Neto, A. Cammarota, L. McShane, and M. Hallett, “Abnormal facilitation of the response to transcranial magnetic stimulation in patients with Parkinson’s disease,” *Neurology*, vol. 44, no. 4, p. 735, 1994.

[24] A. von Leupoldt, A. Keil, P. Y. S. Chan, M. M. Bradley, P. J. Lang, and P. W. Davenport, “Cortical sources of the respiratory-related evoked potential,” *Respir Physiol Neurobiol*, vol. 170, no. 2, pp. 198–201, Feb. 2010, doi: 10.1016/J.RESP.2009.12.006.

[25] A. von Leupoldt, P.-Y. S. Chan, M. M. Bradley, P. J. Lang, and P. W. Davenport, “The impact of anxiety on the neural processing of respiratory sensations,” *Neuroimage*, vol. 55, no. 1, pp. 247–252, 2011.

[26] T. Reijnders *et al.*, “Brain Activations to Dyspnea in Patients With COPD,” *Front Physiol*, vol. 11, no. January, pp. 1–5, 2020, doi: 10.3389/fphys.2020.00007.

[27] M. M. Hoehn and M. D. Yahr, “Parkinsonism,” *Neurology*, vol. 17, no. 5, pp. 427 LP – 427, May 1967, doi: 10.1212/WNL.17.5.427.

[28] A. Delorme and S. Makeig, “EEGLAB: an open source toolbox for analysis of single-trial EEG dynamics including independent component analysis,” *J Neurosci Methods*, vol. 134, no. 1, pp. 9–21, Mar. 2004, doi: 10.1016/J.JNEUMETH.2003.10.009.

[29] J. Lopez-Calderon and S. J. Luck, “ERPLAB: An open-source toolbox for the analysis of event-related potentials,” *Front Hum Neurosci*, vol. 8, no. 1 APR, p. 75729, Apr. 2014, doi: 10.3389/FNHUM.2014.00213/BIBTEX.

[30] A. Von Leupoldt, A. Keil, and P. W. Davenport, “Respiratory-related evoked potential measurements using high-density electroencephalography,” *Clin Neurophysiol*, vol. 122, no. 4, pp. 815–818, Apr. 2011, doi: 10.1016/J.CLINPH.2010.10.031.

[31] S. Vijayan, B. Singh, S. Ghosh, R. Stell, and F. L. Mastaglia, “Dyspnea in Parkinson’s disease: an approach to diagnosis and management,” *Expert Rev Neurother*, vol. 20, no. 6, pp. 619–626, Jun. 2020, doi: 10.1080/14737175.2020.1763795.

[32] P. H. Quanjer *et al.*, “Multi-ethnic reference values for spirometry for the 3–95-yr age range: the global lung function 2012 equations,” *European Respiratory Journal*, vol. 40, no. 6, pp. 1324–1343, Dec. 2012, doi: 10.1183/09031936.00080312.

[33] H. Onodera, S. Okabe, Y. Kikuchi, T. Tsuda, and Y. Itoyama, “Impaired chemosensitivity and perception of dyspnoea in Parkinson’s disease,” *Lancet*, vol. 356, no. 9231, pp. 739–740, Aug. 2000, doi: 10.1016/S0140-6736(00)02638-6.

[34] A. Bhandari *et al.*, “A meta-analysis of the effects of aging on motor cortex neurophysiology assessed by transcranial magnetic stimulation,” *Clin Neurophysiol*, vol. 127, no. 8, pp. 2834–2845, Aug. 2016, doi: 10.1016/J.CLINPH.2016.05.363.

[35] T. Kujirai *et al.*, “Corticocortical inhibition in human motor cortex,” *J Physiol*, vol. 471, no. 1, pp. 501–519, Nov. 1993, doi: 10.1113/JPHYSIOL.1993.SP019912.

[36] N. S. Hopkinson *et al.*, “Corticospinal control of respiratory muscles in chronic obstructive pulmonary disease,” *Respir Physiol Neurobiol*, vol. 141, no. 1, pp. 1–12, Jul. 2004, doi: 10.1016/j.resp.2004.04.003.

[37] J. C. Rothwell and M. J. Edwards, *Brain Stimulation: Chapter 42. Parkinson’s disease*, vol. 116. Elsevier Inc. Chapters, 2013.

[38] K. E. Webster and I. M. Colrain, “The respiratory-related evoked potential: Effects of attention and occlusion duration,” *Psychophysiology*, vol. 37, no. 3, pp. 310–318, May 2000, doi: 10.1111/1469-8986.3730310.

[39] P. W. Davenport, P. Y. S. Chan, W. Zhang, and Y. L. Chou, “Detection threshold for inspiratory resistive loads and respiratory-related evoked potentials,” *J Appl Physiol (1985)*, vol. 102, no. 1, pp. 276–285, Jan. 2007, doi: 10.1152/JAPPLPHYSIOL.01436.2005.

[40] I. Epiu *et al.*, “Respiratory-related evoked potentials in chronic obstructive pulmonary disease and healthy aging,” *Physiol Rep*, vol. 10, no. 23, Dec. 2022, doi: 10.14814/PHY2.15519.

[41] R. Cantello, M. Gianelli, D. Bettucci, C. Civardi, M. S. De Angelis, and R. Mutani, “Parkinson’s disease rigidity: magnetic motor evoked potentials in a small hand muscle,” *Neurology*, vol. 41, no. 9, pp. 1449–1456, 1991, doi: 10.1212/WNL.41.9.1449.

Appendix A: Neural control of breathing

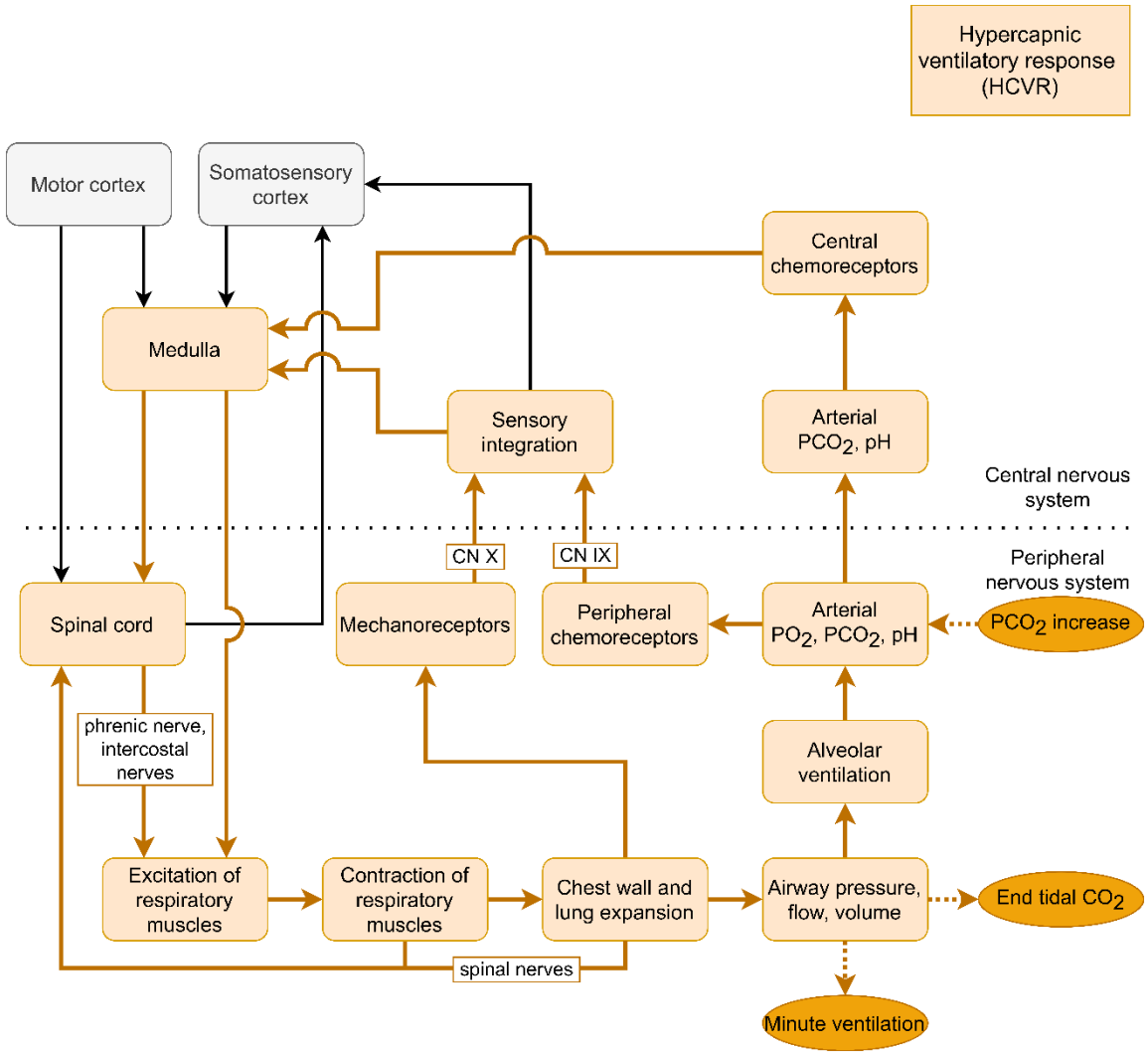

Figure 12 Neural control of ventilation. The pathway that is assessed with the hypercapnic ventilatory response is indicated in orange. The input and output parameters of the measurement are indicated with darker orange. CN X: vagal nerve, CN IX: glossopharyngeal nerve, PCO2: partial pressure of carbon dioxide, PO2: partial pressure of oxygen.

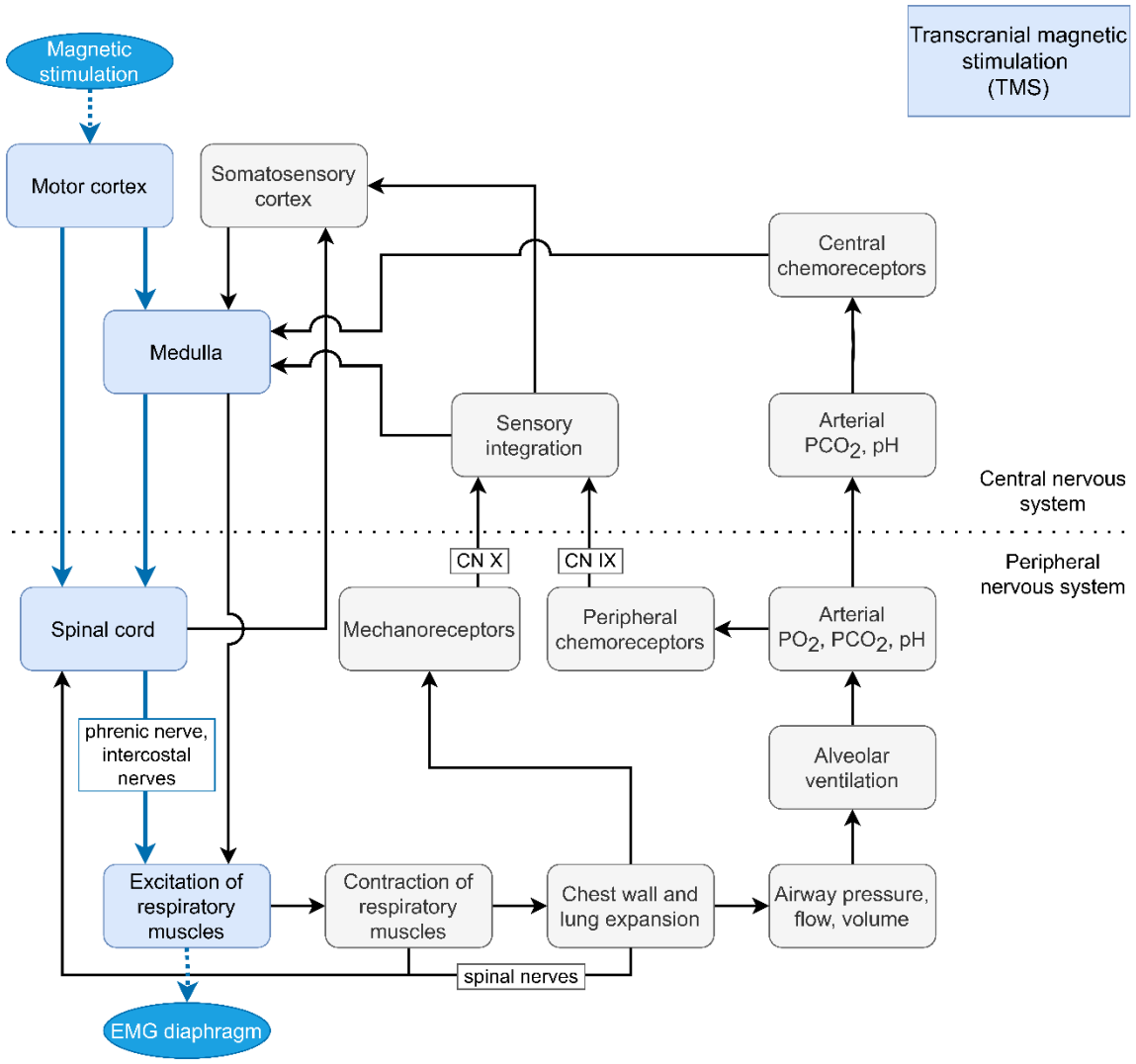

Figure 13 Neural control of ventilation. The pathway that is assessed with the transcranial magnetic stimulation is indicated in blue. The input and output parameters of the measurement are indicated with darker blue. CN X: vagal nerve, CN IX: glossopharyngeal nerve, PCO2: partial pressure of carbon dioxide, PO2: partial pressure of oxygen, EMG: electromyography.

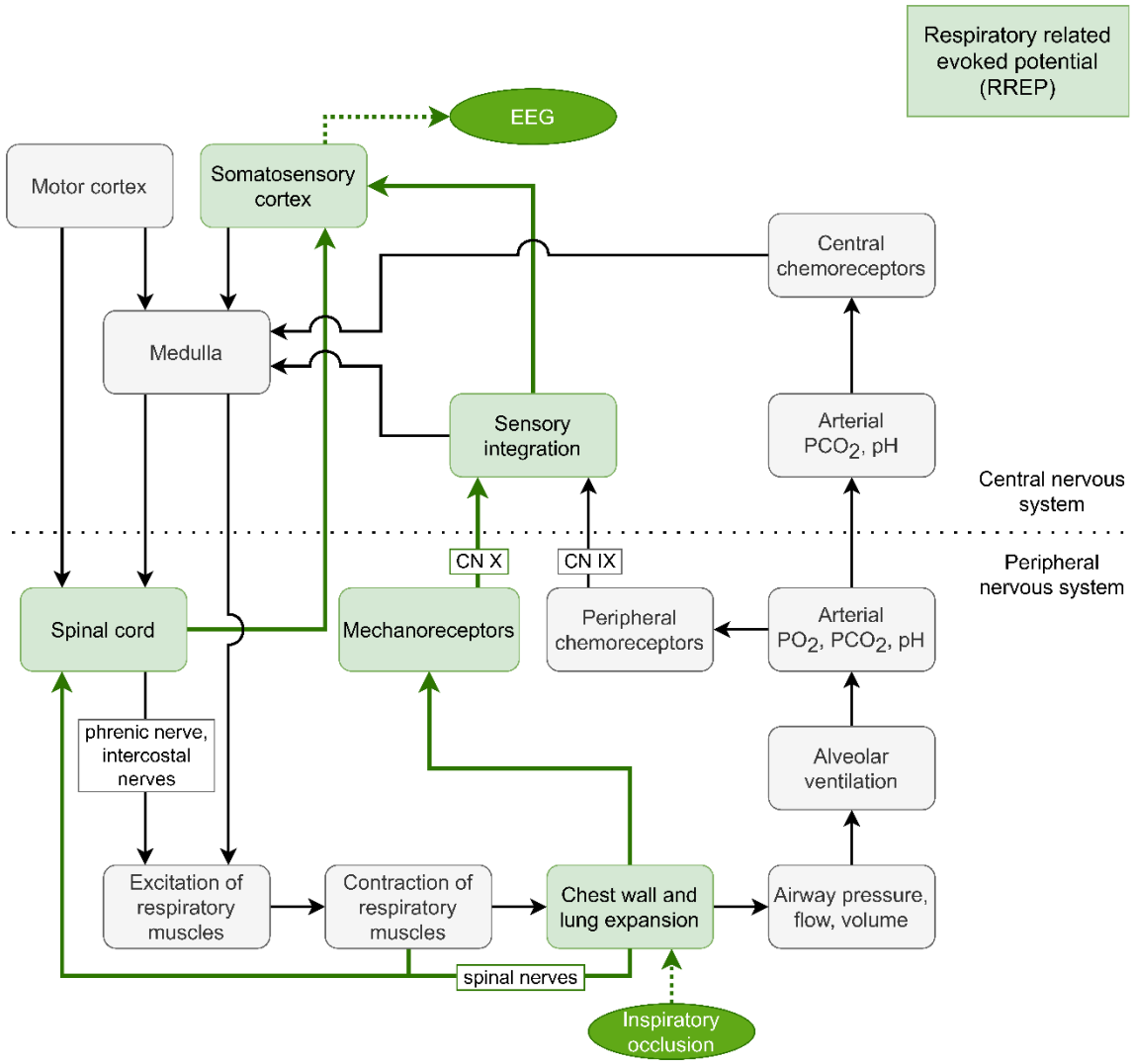

Figure 14 Neural control of ventilation. The pathway that is assessed with the transcranial magnetic stimulation is indicated in blue. The input and output parameters of the measurement are indicated with darker blue. CN X: vagal nerve, CN IX: glossopharyngeal nerve, PCO2: partial pressure of carbon dioxide, PO2: partial pressure of oxygen, EEG: electroencephalography.

Appendix B: Additional results

Subject characteristics

Table 7 Subject characteristics for each subject individually. Healthy controls (HC) and subjects with Parkinson's disease (PD) are presented.

Subject	Group (HC/PD)	Age (years)	Sex	BMI (kg/m^2)	History of smoking	Duration of disease (years)	Hoehn & Yahr stadium
HC1	HC	24	Female	20.3	No	-	-
HC2	HC	33	Female	34.7	Yes	-	-
HC3	HC	30	Female	24.2	No	-	-
HC5	HC	52	Female	28.7	No	-	-
HC4	HC	43	Female	22.3	No	-	-
HC6	HC	61	Male	27.7	Yes	-	-
HC7	HC	67	Male	24.9	Yes	-	-
HC8	HC	32	Male	29.9	No	-	-
HC9	HC	58	Female	27.4	No	-	-
PD1	PD	67	Male	27.4	Yes	4.5	2.5
PD2	PD	61	Male	23.0	No	5	2
PD3	PD	64	Female	20.1	No	4	2
PD4	PD	66	Male	26.3	No	2.5	3
PD5	PD	66	Male	23.9	No	8.5	3

Pulmonary function

Table 8 Pulmonary function for each subject individually.

Subject	FEV_1 (%pred)	FVC (%pred)	FEV_1/FVC	MIP (%pred)	MEP (%pred)	SNIP (%pred)
HC1	97	91	0.91	119	103	80
HC2	97	92	0.84	165	121	176
HC3	102	96	0.88	116	82	104
HC5	82	80	0.84	138	86	104
HC4	109	114	0.77	177	148	141
HC6	111	111	0.84	88	117	93
HC7	90	101	0.69	126	108	79
HC8	106	116	0.71	177	128	110
HC9	83	98	0.66	129	135	125
PD1	91	105	0.66	132	106	102
PD2	90	95	0.72	103	132	66
PD3	113	119	0.74	99	112	91
PD4	110	117	0.71	123	91	64
PD5	132	135	0.74	71	72	-

FEV_1: forced expiratory volume in 1 second, FVC: forced vital capacity, MIP: maximal inspiratory pressure, MEP: maximal expiratory pressure, SNIP: sniff nasal inspiratory pressure. All parameters, except the ratio of FEV1 and FVC, are shown as a percentage of the predicted value for that individual.

Respiratory related evoked potential

Table 9 Latencies and amplitudes for the components of the respiratory related evoked potential (RREP) for healthy controls (HC) and subjects with Parkinson's disease (PD).

RREP component	Latency (ms)		Amplitude (µV)	
	HC	PD	HC	PD
NF	60	60	-1.78	-0.91
P1	60	100	0.52	0.28
N1	160	220	-0.09	-0.02
P2	340	308	3.43	1.15
P3	408	472	3.90	2.19